N71-34993

RI 7543

Bureau of Mines Report of Investigations/July 1971

CASTLE COPY

Gravity Flow of Powder in a Lunar Environment

(In Two Parts)

1. Property Determination of Simulated Lunar Soil

UNITED STATES DEPARTMENT OF THE INTERIOR

Report of Investigations 7543

Gravity Flow of Powder in a Lunar Environment

(In Two Parts)

1. Property Determination of Simulated Lunar Soil

By David E. Nicholson

UNITED STATES DEPARTMENT OF THE INTERIOR
Rogers C. B. Morton, Secretary

BUREAU OF MINES
Elburt F. Osborn, Director

This publication has been cataloged as follows:

Nicholson, David E

Gravity flow of powder in a lunar environment. (In two parts.) 1. Property determination of simulated lunar soil. [Washington] U.S. Dept. of the Interior, Bureau of Mines [1971]

34 p. illus., tables. (U.S. Bureau of Mines. Report of investigations 7543)

Includes bibliography.

1. Lunar soil. 2. Bins. 3. Materials handling. I. Title. II. Title: Lunar-basalt powder, Simulated. (Series)

TN23.U7 no. 7543 622.06173

U.S. Dept. of the Int. Library

CONTENTS

	Page
Abstract	1
Introduction	1
Lunar environment	2
Lunar-soil material	2
Effects of lunar environment on the properties of lunar materials	3
Acknowledgments	4
Gravity flow from bins: historical background	4
Simulation of the lunar-soil matrix	6
Description of experimental work	10
Direct-shear testing of simulated lunar soil	10
Wall-friction tests	11
Torsional-shear tests	12
One-dimensional compression earth-pressure-at-rest tests	19
Summary and conclusions	30
References	32
Appendix	34

ILLUSTRATIONS

1.	Conceptual gravity-flow bin	5
2.	Grinding circuit for the production of simulated lunar soil	7
3.	Photomicrograph of simulated lunar soil	8
4.	Grain-size distribution of simulated lunar soil and the soil matrix recovered from the Apollo-11 mission	9
5.	Peak-failure envelope of direct- and torsional-shear tests for normally consolidated, simulated lunar soil	10
6.	Simulated lunar soil-steel wall friction test results	11
7.	Detail drawing: torsional-shear tester	14
8.	Vacuum torsional-shear tester (TCMRC)	15
9.	Earth-atmosphere torsional-shear tester (SMRC)	16
10.	Calibration of the torsional-shear tester	17
11.	Torsional test graph of shear load and normal load	18
12.	Results of torsional-shear tests on simulated lunar soil at 45.5 g/cm^2 consolidation	20
13.	Results of torsional-shear tests on simulated lunar soil at 69.8 g/cm^2 consolidation	21
14.	Results of torsional-shear tests on simulated lunar soil at 91.0 g/cm^2 consolidation	22
15.	Flow-function of simulated-soil matrix from torsional-shear tests	23
16.	One-dimensional compression K_o chamber	24
17.	K_o chamber prior to assembly	25
18.	K_o stress ratio versus overconsolidation ratio for sand at various initial void ratios	26
19.	K_o chamber and data-acquisition system	29
20.	Load-displacement curve for simulated lunar soil from K_o compression test	30

TABLES

Page

1. Comparative physical properties of simulated lunar-soil and the Apollo-11 core tube samples..... 9
2. Earth-pressure-at-rest compression tests on simulated lunar soil..... 28

GRAVITY FLOW OF POWDER IN A LUNAR ENVIRONMENT

(In Two Parts)

1. Property Determination of Simulated Lunar Soil

by

David E. Nicholson [1]

ABSTRACT

This report investigates the mechanical behavior of fine soils in a lunar environment in engineering gravity-flow bins. The ultrahigh vacuum, absence of moisture, and a lunar gravity one-sixth that of earth gravity represents a unique environment, both advantageous and detrimental to these systems. On earth, moisture and gases contained in powder masses can be responsible for complex descriptions of gravity flow. Their absence appear to simplify the lunar soil behavior. However, simulation of the lunar gravity and vacuum complicates the development of experimental data for designing bins.

The properties of a dry soil powder, its behavior under one-dimensional compression, and its torsional and direct shearing strength under earth atmosphere are described in part 1 of this paper. These properties provide the parameters for a finite-element analysis to optimize the design of bins, to be described by Dr. William Pariseau in part 2.

Shear tests assess the failure criteria for the material. Compression tests provide modulus and (K_o) stress-ratio values from the loading portion of the compression cycle, duplicating the condition of a bin at rest with the discharge closed. During the unloading portion of the compression cycle (soil overconsolidated), the residual K_o values rise. It is postulated that this phenomenon creates a high-lateral stress in bins when they approach incipient flow. Assessment of the K_o value, overconsolidation ratio, and the void ratio state is proposed as a criterion to determine the flowability of powder.

INTRODUCTION

The U.S. Bureau of Mines is engaged in a research program to acquire fundamental scientific and engineering knowledge of lunar-mineral resources for NASA's Office of Advanced Research and Technology (1).[2] This program envisions the utilization of lunar soil or rock materials to support future manned

[1]Mining engineer, Spokane Mining Research Center, Bureau of Mines, Spokane, Wash.

[2]Underlined numbers in parentheses refer to items in the list of references preceding the appendix.

space missions. As part of this investigation, the Spokane Mining Research Center (SMRC) has been assigned the exploration or problems associated with the handling and stowage of fine particulate materials on the moon. Of particular interest--and the primary project task--has been the study of gravity flow of fine lunar-soil aggregations from storage bins.

The project work was initiated in 1967, before the first Surveyor spacecraft landing, so that many important research decisions were based on speculative and postulate reasoning, and upon whatever information could be interpreted from the early Surveyor landing experiments. In retrospect, these decisions--such as duplication of the fine-particle size fraction of the lunar soil, which could not be resolved in the Surveyor-mission photographs--seem almost inconsequential. Initially, however, the lack of definitive basis for judgment caused great difficulty, because research had to be guided by deduction and extrapolation.

Lunar Environment

This environment is characterized by ultrahigh vacuum pressure ranging from 10^{-10} to 10^{-12} torr. Because of the direct radiation from the sun, lunar-surface temperatures swing from extreme heat (+135° C) during the day, to extreme cold (-130° C) during the lunar night. The surface is also exposed directly to the so-called solar wind, composed of streams or a plasma of high-energy nuclear particles emanating from the sun. Probably the most significant environmental influence, insofar as it affects the gravity flow of fine particulate matter, is the reduced lunar-gravity field. The influence of these environmental characteristics will be considered later in this report.

Lunar-Soil Material

A considerable portion of the lunar surface was known to be covered by a fine granular material. This soillike substance has a distinct advantage as a potential resource material, since it is essentially comminuted, and its utilization would require only collection, minor classification, and a workable storage system. It was hypothesized that this regolith is principally debris from meteoric impacts, with some possibility of admixed clastic material, deposited through many geological eons by volcanic eruptions through the lunar crust. Both processes were assumed to have produced a rather angular, siltlike soil matrix. Surveyor spacecraft photographs could not resolve the fine portion of this lunar soil, so that an exact-size distribution could not be predicted. Nevertheless, the photographs did allow selective cumulative counts and sizing of the large fragments (9). By assuming an approximate semilogarithmic size distribution, and by estimating (rational conjecture) the total number of particles within a unit area of surface, we were able to extrapolate the coarse particle-size distribution to simulate the fine portion (<1 mm diam) of the lunar soil.

In addition to photographic data from the Surveyor landings, a nuclear alpha-scattering instrument analyzed the chemical composition of the regolithic surface (9). These experiments consistently indicated a basaltlike soil material with a significant percentage of oxygen. An electromagnetic

experiment showed that only minor amounts of magnetic material (<0.25 percent) were contained in the lunar soil, whereas a soil-trenching experiment (carried on by the earlier Surveyor spacecraft) and analysis of footpad impressions revealed a loosely structured lunar-soil matrix with mild cohesion.

Effects of Lunar Environment on the Properties of Lunar Materials

Of principal importance to the research project was the influence of the lunar environment on the handling properties of soil materials. It was speculated that the high vacuum might produce ultraclean particle surfaces, making the lunar material self-binding or highly cohesive, an effect principally of molecular attraction. Others felt that the particle surface would be contaminated with partial or complete monolayers of gas molecules, irrespective of the high lunar vacuum. However, Surveyor trenching in the in situ soil seemed to discover only a mild cohesion in a state analogous to fine, moist earth soil, with particle coherence due to surface tension. This observation tended to support the idea of some self-contamination or a reduced importance of the molecular forces influencing vacuum cohesion.

Gravity forces acting on the moon, about one-sixth those of earth, have a pronounced influence on the development of gravity flow and rate of flow from bins and hoppers. Hence, the lunar force field was expected to have significant influence on the consolidation of the lunar material, reducing the stresses that cause gravity flow out of a bin storage unit, and also changing the critical void-ratio confining pressure relation at which a granular material's dilatency (volume expansion) characteristics are mobilized in shearing or compression (19). Thus, a typical powder material was expected to retain a higher void-ratio state when placed freely in a bin or container on the moon. Offsetting to a minor degree the influence of the lunar-gravity field, and reducing the weight of the particulate matter (and thereby the gravity stresses), was the elimination--in the lunar vacuum--of any atmospheric buoyancy effect on the mass weight of the particulate material.

Again, although our knowledge of the lunar-surface material and the influence of the lunar environment was mainly deductive, certain general assumptions seemed valid:

1. An earth-basalt rock with mild magnetic properties would be used as a standard for the lunar soil-powder simulation.

2. An impact milling method would be developed to produce an angular, siltlike rock powder, which would be classified to a well-graded grain-size distribution--similar to the distribution postulated from the Surveyor spacecraft photographs.

3. Physical-property testing would need to reflect the low stresses (due to reduced gravity) developed in these soil masses. Needed also would be a special shear-testing device adaptable to testing in an ultrahigh vacuum system.

4. It is speculated that temperature extremes, particle erosions from solar-wind bombardment, and the lack of atmospheric buoyancy have only a minor influence. Thus these variables could be eliminated from the initial research.

ACKNOWLEDGMENTS

Work on the project, in both the development of special testing apparatus and the performance of various tests, required the dedicated efforts of many individuals. Mr. Robert Warner, Warner Machine Works, Spokane, Wash., constructed the first working model of the torsional-shear tester and installation of instrumentation on the one-dimensional compression chamber. Laboratory tests with the latter were principally performed by Howard Pettibone, Civil Engineer, at the Spokane Mining Research Center, and Michael Strom, engineering technician at the laboratory, conducted the direct-shear tests, grain-size analysis, and physical-property tests.

Preliminary editorial review has been performed by Mr. William Chance, Spokane Mining Research Center, Spokane, Wash., and scientific review by Professor Robert Schuster, University of Idaho, Moscow, Ida.

GRAVITY FLOW FROM BINS: HISTORICAL BACKGROUND

Early theoretical and experimental work on pressure distribution, and on the flow of granular solids from prismatic bins and vertical walled silos, was done by Janssen (1895), Koenen (1896), Airy (1897), and Kötter (1899). Karl Terzaghi presents a general review of these early investigations under "Theories of Arching" (18). Application of these theories and empirical methods apparently dominated bin-design engineering for many years.

In 1961, Andrew Jenike (5) initiated the modern trend in bin engineering by applying soil-mechanics principles to the gravity-flow-of-bulk solids. Briefly, Jenike developed special shear-testing methods to ascertain unconfined strengths of overconsolidated granular materials and to discover an "Effective Angle of Internal Friction" (6). The state of stress in a gravity bin with converging channel is defined by Jenike in a form analogous to that of the Rankine coefficient of active earth-pressure. A solution is obtained by translation of the principal stress by assuming a uniform radial stress field near the discharge orifice, from which a flow-factor is calculated to optimize the design of the bin. Applications of Jenike's methods are further documented in recent papers (6-8). More recently, Walker in 1967 proposed a method of ring or torsional-shear testing of fine coal powder for bin-flow analysis (21). Working with experimental coal bunkers, Walker also developed an alternate flowability analysis for the British Central Electricity Generating Board (20). Utilizing the Jenike direct-shear apparatus, Williams and Birks (22) also proposed improved methods for testing fine-powder materials. The work of these experimenters gave the principal impetus and direction to our subsequent research on bin flow.

Lacking a clear definition of the bin stress field, and faced with a significant conflict between the Jenike and Walker methods of deriving the so-called Flow-Factors for bin design (20), it was decided that a more

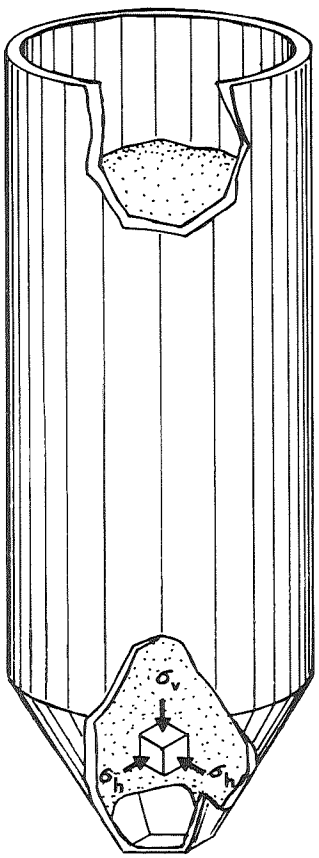

GRAVITY FLOW BIN

K_o STRESS ELEMENT

$K_o = \frac{\sigma_h}{\sigma_v}$

AT REST $\sigma_v > \sigma_h$

AT INCIPIENT FLOW $\sigma_h \cong \sigma_v$

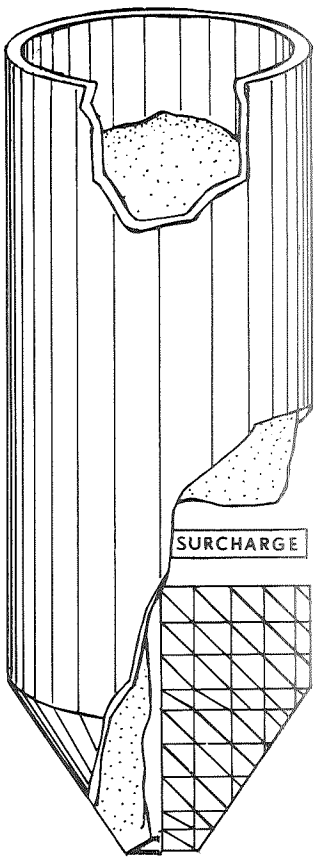

GRAVITY FLOW BIN

FINITE-ELEMENT MESH

REQUIRED FOR SOLUTION	1. Modulus of element 2. Poisson ratio 3. Boundary wall friction 4. Failure criteria for material (Mohr-Coulomb)
OPTIMIZE SOLUTION FOR FLOW	1. Outlet size 2. Bin wall slope 3. Height of bin

FIGURE 1. - Conceptual Gravity-Flow Bin.

elementary, less restrictive approach to the classical bin-flow problem was justified. Thus, it was proposed to analyze the involved bin-flow problem by computer finite-element methods, which were originally developed by Zienkiewicz to solve structural-mechanics problems (23). Complex mine structural problems had previously been analyzed at the Spokane laboratory by the finite-element technique; too, an earth-pressure-at-rest, one-dimensional compression chamber was available to determine both a deformation or secant modulus and various principal stress-ratio values needed in exploiting the finite-element technique. Figure 1 illustrates a conceptual gravity bin with a basic stress-element, and an adjacent view showing an example of a finite-element mesh to be used for analysis.

In summary, gravity-flow research would not only utilize (or adapt) most of the shear-strength testing methods for granular materials, but would also develop secant moduli and stress ratio values to define the stress states in gravity bins. Thus, we could avoid making complex assumptions about the stress field and perform a flow analysis directly with finite-element methods.

SIMULATION OF LUNAR-SOIL MATRIX

It was decided to replicate the lunar-soil matrix by producing a rock powder from fresh rock samples. Guided by Surveyor chemical-analysis data, a large sample of basalt rock was collected from a tholeiitic flow of the Columbia River Basalt in central Oregon. This flow basalt is one of a group of rocks proposed by geologists as a potential simulator of the lunar rock crust. Its physical and chemical properties have been reported in detail by Fogelson (2). The sample was reduced and classified in a special grinding circuit, set up at the laboratory (fig. 2).

To reduce the material to a nominal 1/8-inch size, it was first fed to a standard gyratory crusher, and then to a special cone-type gyratory roll crusher. The crusher product passed over a vibrating 1/8-inch screen, and the undersize was fed to a 20,000-rpm, high-speed impact mill. This process was intended to duplicate, to some degree, the high-energy mechanism of meteoric impacts that created most of the lunar-soil debris. From the impact mill, the material (now rock powder) was carried by airflow in special tubing directly to a special 12-inch-diameter air cyclone, which recovered the powder from the airstream and classified the final sample. A photomicrograph (fig. 3) shows the angular, siltlike particles produced from the impact mill grinding.

The grain-size distribution, determined by screen and hydrometer analysis of the basalt powder used to simulate the lunar soil is shown in figure 4 along with the grain-size analysis obtained later from the Apollo-11 lunar soil samples returned to earth (10). The grain-size distribution of the two materials is seen to match reasonably well except at the uppermost coarse-size fractions, which in any event would be removed from the sample prior to soil

FIGURE 2. - Grinding Circuit for the Production of Simulated Lunar Soil.

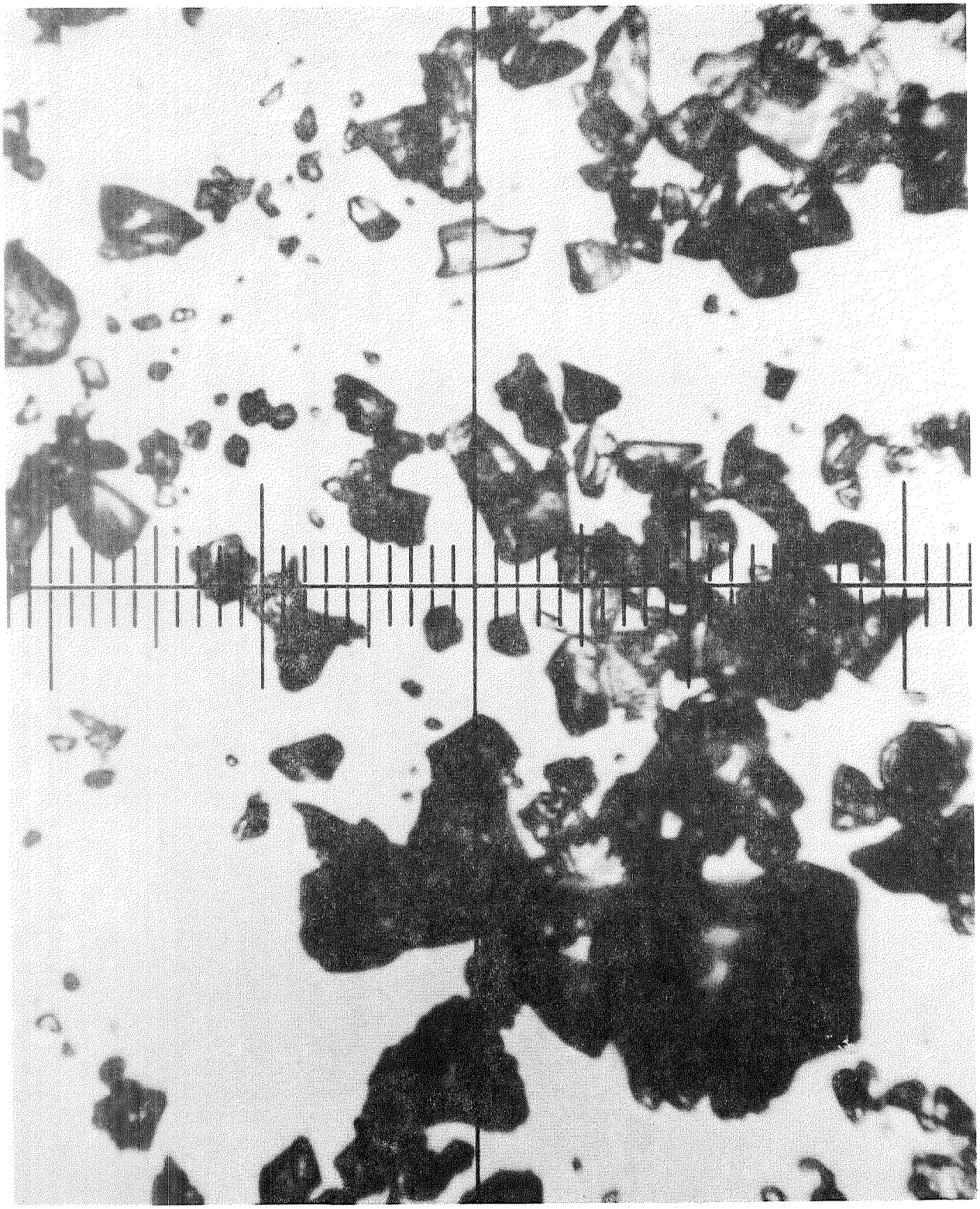

FIGURE 3. - Photomicrograph of Simulated Lunar Soil.

physical-property tests. Table 1 compares bulk properties of the simulated soil and core-tube samples obtained from the Apollo-11 mission (10). Thus, insofar as seemingly possible, the simulated lunar soil properties closely correlate with the actual lunar-soil matrix, as indicated from the core samples. However, differences in the mineralogical compositions and specific gravity of the two materials are to be noted (10). Also, small beadlike, spherical glass particles, which constitute an estimated 10 to 20 percent of the in situ lunar soil, are not present in the simulated lunar soil.

TABLE 1. - Comparative physical properties of the simulated lunar-soil and the Apollo-11 core tube samples

	Void ratio (e)	Specific gravity (G)	Bulk density (γ), lb/ft^3
Apollo-11 core tube 1.....	0.87 (in situ)	3.1	103
Apollo-11 core tube 2.....	1.01 (in situ)	3.1	96
Simulated soil (basalt powder)..	1.02 (lab min.)	2.9	90

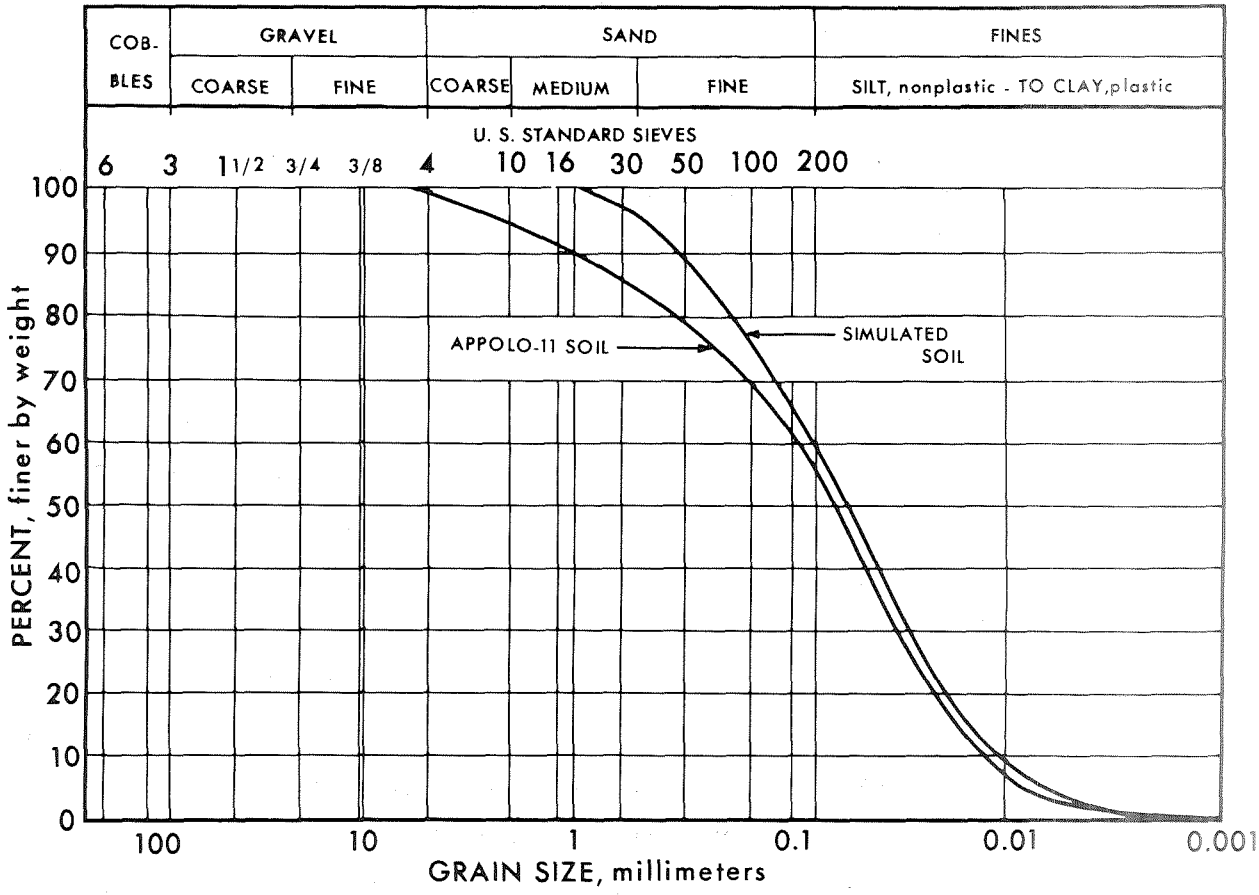

FIGURE 4. - Grain-Size Distribution of Simulated Lunar Soil and the Soil Matrix Recovered From the Apollo-11 Mission.

DESCRIPTION OF EXPERIMENTAL WORK

Direct-Shear Testing of Simulated Lunar Soil

A series of direct-shear tests were run on oven-dried simulated lunar soil under normal earth-atmosphere conditions, employing a standard, direct-shear machine. Normal loads are applied through a lever-arm, deadweight (inertial) system. The nominal load range of this machine is higher than the gravity loads expected in gravity-bin design. The principal usefulness of the direct-shear tests was to supplement and extend data obtained by shearing tests at lower loads (performed on a special torsional-shear device), which will be discussed later. Loose samples of simulated lunar soil were normally consolidated, and only a peak shear strength was obtained from these direct-shear tests. Figure 5 shows the results of this test series and also data from torsional tests, both of which define a peak Mohr failure envelope for the loose, normally consolidated basalt powder.

A linear graphical representation of the Mohr failure envelope (not necessarily the real failure envelope) indicates an angle of internal friction (ϕ) of 35.5° and a shear-axis intercept (c) of 20 g/cm^2 for the simulated lunar-soil matrix. It is of interest that Apollo 11 and 12, soil-mechanics investigations estimate, for the in situ lunar-soil material, a cohesion of about 14 g/cm^2 and angles of internal friction of 35° or greater (10-11). Thus, the shear-strength properties (friction and cohesion) of the basalt powder tested under normal earth-atmospheric conditions, with atmospheric vapor and air gases adhered to the particle surfaces, seem to approximate the gross strength properties of the in situ lunar-soil material in the lunar vacuum.

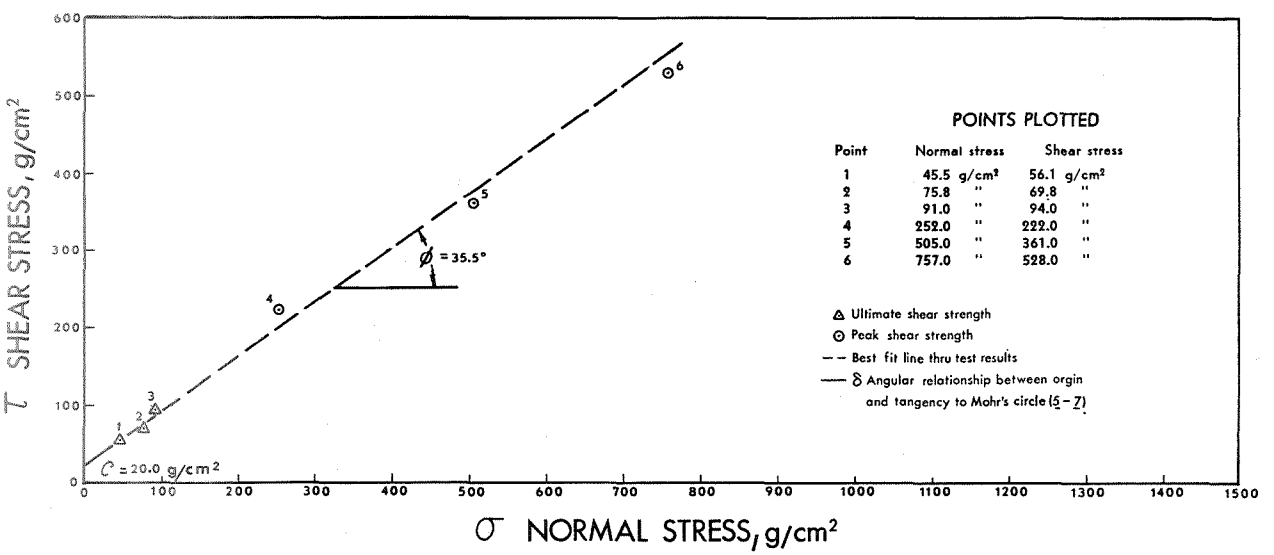
τ SHEAR STRESS, g/cm²
σ NORMAL STRESS, g/cm²
C = 20.0 g/cm²
φ = 35.5°
POINTS PLOTTED
Point Normal stress Shear stress
1 45.5 g/cm² 56.1 g/cm²
2 75.8 " 69.8 "
3 91.0 " 94.0 "
4 252.0 " 222.0 "
5 505.0 " 361.0 "
6 757.0 " 528.0 "
Δ Ultimate shear strength
⊙ Peak shear strength
– – Best fit line thru test results
—— δ Angular relationship between orgin and tangency to Mohr's circle (5 – 7)

FIGURE 5. - Peak-Failure Envelope of Direct- and Torsional-Shear Tests for Normally Consolidated, Simulated Lunar Soil.

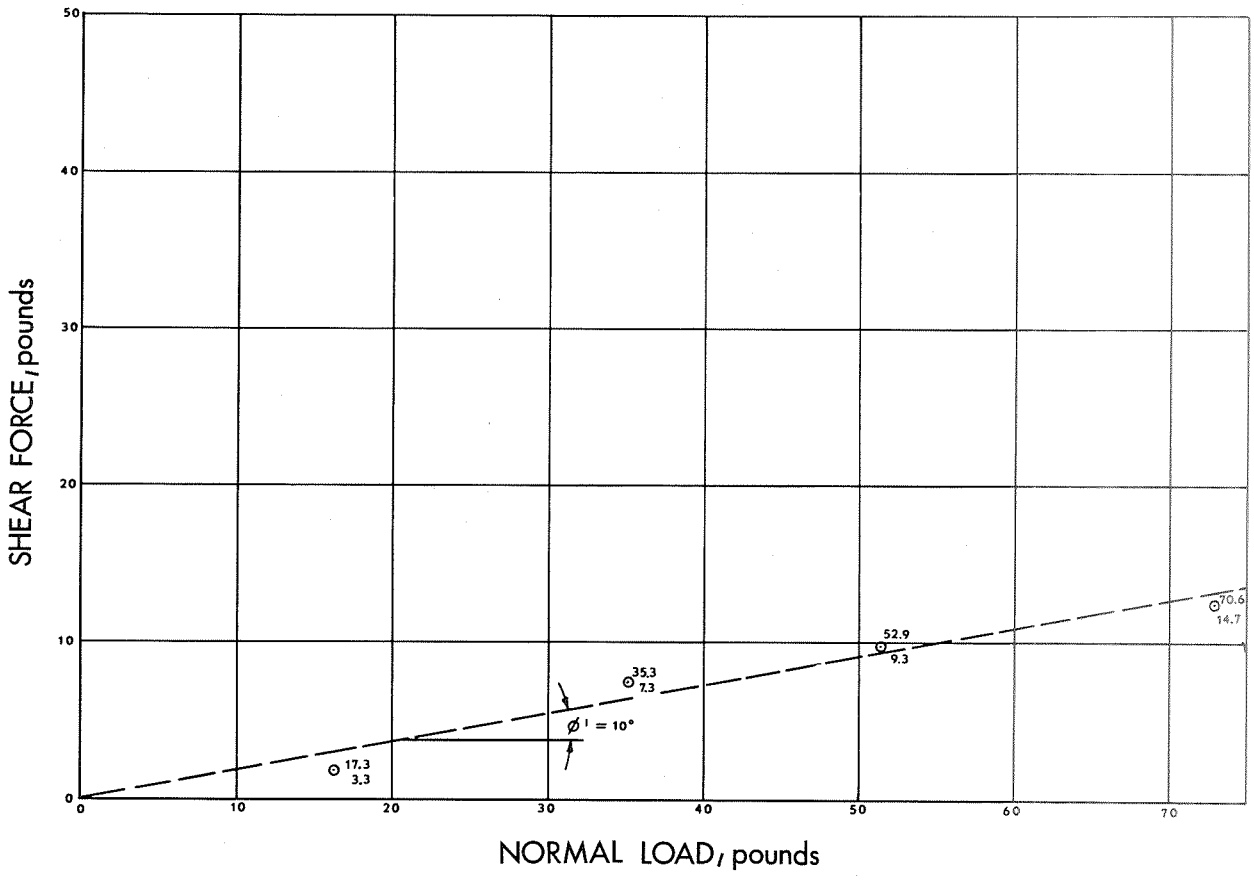

FIGURE 6. - Simulated Lunar Soil-Steel Wall Friction Test Results.

Wall-Friction Tests

The solution of any bin gravity-flow problem requires the determination of a coefficient of friction between the metal wall and the granular material when it is consolidating or flowing in the bin. Following the standard direct-shear machine method utilized by Jenike (7) to determine wall friction, a steel platen insert was made, which was contained in the lower half of the shear box; whereas the upper half of the box was fitted with a Teflon[3] gasket, resting on the steel platen surface and providing near frictionless contact between the shear boxes. The upper half of the shear box was filled with loosely packed basalt powder. The frictional resistance force was measured under several normal loads. Results, plotted in figure 6, indicate an angle of wall friction (ϕ') of 10° between the loose basalt powder and the steel platen material. This friction parameter developed for the sloping bin wall is incorporated into the finite-element analysis as a special boundary condition.

[3]Reference to specific products is made for identification only and does not imply endorsement by the Bureau of Mines.

Torsional-Shear Tests

A predominant project objective was to study the influence of lunar vacuum on the cohesion or fusion of the fine basalt used to simulate the lunar-soil matrix. From a series of one-dimensional compression tests, performed early in the project and discussed in detail later, it was observed that, under earth-atmosphere conditions, a high degree of apparent cohesion occurs in the simulated basalt soil powder (13). Consequently, it was inferred that any cohesion due to molecular attractions in the lunar vacuum would not, in a relative sense, greatly affect the strength parameters of the lunar soil employed for the analysis of bin flow. However, this supposition was to be proved or disproved only by actually developing a suitable shear-testing procedure and performing shear tests in an extremely complex ultrahigh-vacuum testing program capable of reducing chamber pressure to near 10^{-12} torr.

Moreover, the research proposed to examine relative increases in cohesion with consolidation pressures in both atmosphere and in vacuum; comparison of the data would indicate the relative influence of vacuum on the powder cohesion and strength. The lunar soil, which would be classified as a dry cohesionless, fine sandy silt, would thus be shear-tested in a manner normally reserved in soil mechanics for studying consolidated, saturated clay materials, such as those proposed by Krey-Teidemann, Hvorslev, and Bjerrum (19). The effect of consolidation on soil cohesion (and dilatency) has been recently explored by Roscoe and coworkers (16) and Palmer and coworkers (14). In their work on bin flow, Jenike (5, 7) and Walker (21) treat fine granular materials in an analogous manner: by determining their "flow functions." As shown in figure 15, flow function may be defined as the ratio of the unconfined yield strength to principal preconsolidating stress.

As Tschebotarioff (19) has stated, it is important to consider that this type of failure criterion abandons the classical concept of cohesion as having a constant value for a given material; rather, the indication is that it is strongly influenced by the preconsolidation load. This distinction obscures the conventional clear-cut separation between friction and cohesion in Mohr-Coulomb materials, whether they be true cohesive clays or simply dilative, cohesionless materials under extremely low loads, as in gravity-flow bins.

Vacuum testing of the simulated lunar soil requires that numerous individual tests be performed, both at various ranges of consolidation load and at various states of overconsolidation. Ideally, these shear tests should check both the peak and ultimate shear strength. Thus, a direct-shear method was ruled out, since preparation and pumpdown of the vacuum systems would require several weeks, whereas a single shear test would require, at most, 15 minutes of testing time.

A torsional-shear device with infinite rotational displacement was thus devised, which overcame the major objection to direct shear, in that a single sample could be continuously tested, under a variety of states of consolidation and overconsolidation, without reentering the vacuum system. Further, the torsional-shear tester, having infinite shear-strain potential, made possible observation of both the peak and ultimate shear strengths of basalt

powder in a single test. In many respects, the torsional method is preferable to the direct-shear method, in that it requires no special sample preparation since the infinite shear-strain potential allows determination of the ultimate powder shear strength. Figure 7 shows the detail drawing of the torsional tester as finally developed. Two models were constructed: one for vacuum testing, which is being performed at the Bureau's Twin Cities Mining Research Center (TCMRC) in a special ultrahigh vacuum system and described by Roepke (15); a second tester was constructed at the Spokane Mining Research Center (SMRC) for normal atmosphere testing, where the general test procedure could be refined under less difficult conditions, preceding the vacuum test work. The vacuum-testing phase is on-going research, which will be reported at a later date. Figure 8 illustrates the tester mounted in the TCMRC vacuum system; an assembled view of the normal atmosphere tester at SMRC is showed in figure 9.

In both testers, a ring-shaped sample is formed in the chamber, to minimize the variable shear strain across the shear surface of the sample. A cantilever-beam system supports the sample chamber base. The normal load, applied by the vane head, is read out on four cantilever beam supports, gaged top and bottom with strain gages. To maximize strain and minimize deflection, these beams are short and constructed of low-modulus aluminum. The eight-active-gage configuration used in the normal-load bridge circuit averages the normal force applied to the sample chamber.

Normal loads, applied by the vane head, act through compression springs of a predetermined stiffness of 2,000 g/cm. This stiffness has been derived as a crude static approximation of the stiffness of the simulated soil matrix, by utilizing the soil spring constant formula (18) and by incorporating the stress-strain properties of the simulated lunar soil as determined from the one-dimensional compression tests. Thus, as the basalt powder is shearing, the restraint of the spring mechanism is approximately equivalent to the restraint produced by the powder mass as it dilates. Because of the relative decrease in frictional resistance and an increase in the volume-expansion characteristics of the basalt powder under low normal stresses, this feature in the design of the torsional-shear tester is believed to be of particular importance for testing materials for gravity-flow analysis.[4]

Shearing stresses are measured by a cantilever-beam transducer contained in the torque head. These beams are made from cold-rolled, copper-beryllium alloy, and instrumented with four active strain gages. When the vane head is pressed into the sample and the shaft drive is turned, shear stresses produce bending in the four cantilever beams, a consequence of the shear resistance of the basalt powder material. Shear stresses in the basalt powder are determined from the "center of mass" of the wedge-shaped shear surface contained within each pair of vanes. This distance is calculated as 1.429 inches from the axis of rotation, which is the radius distance of each compression spring shaft from this axis.

[4] In the context of direct-shear testing of consolidated saturated clays, both Palmer (14) and Tschebotarioff (19) indicate the influence of normal restraint on soil-strength properties.

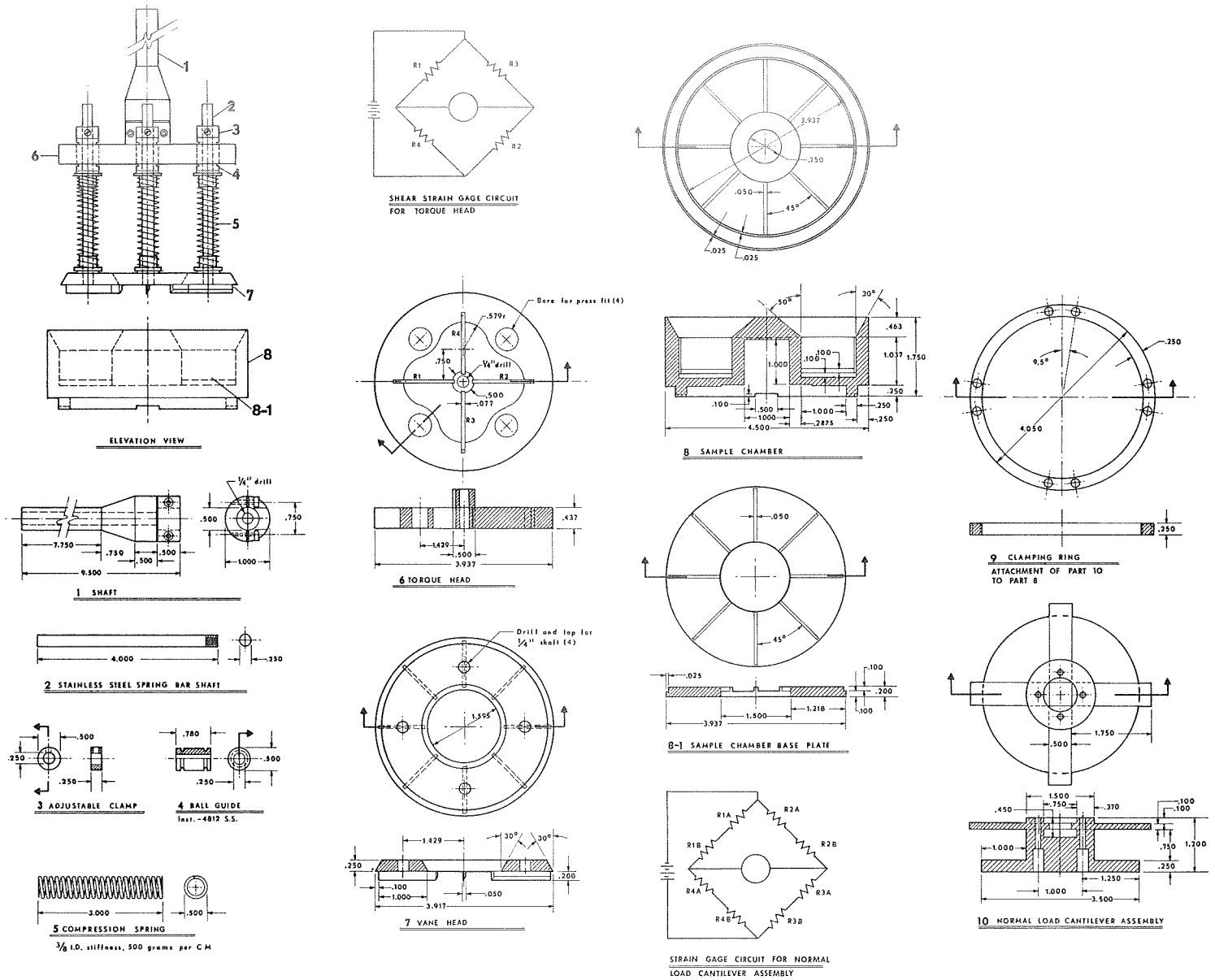

FIGURE 7. - Detail Drawing: Torsional-Shear Tester.

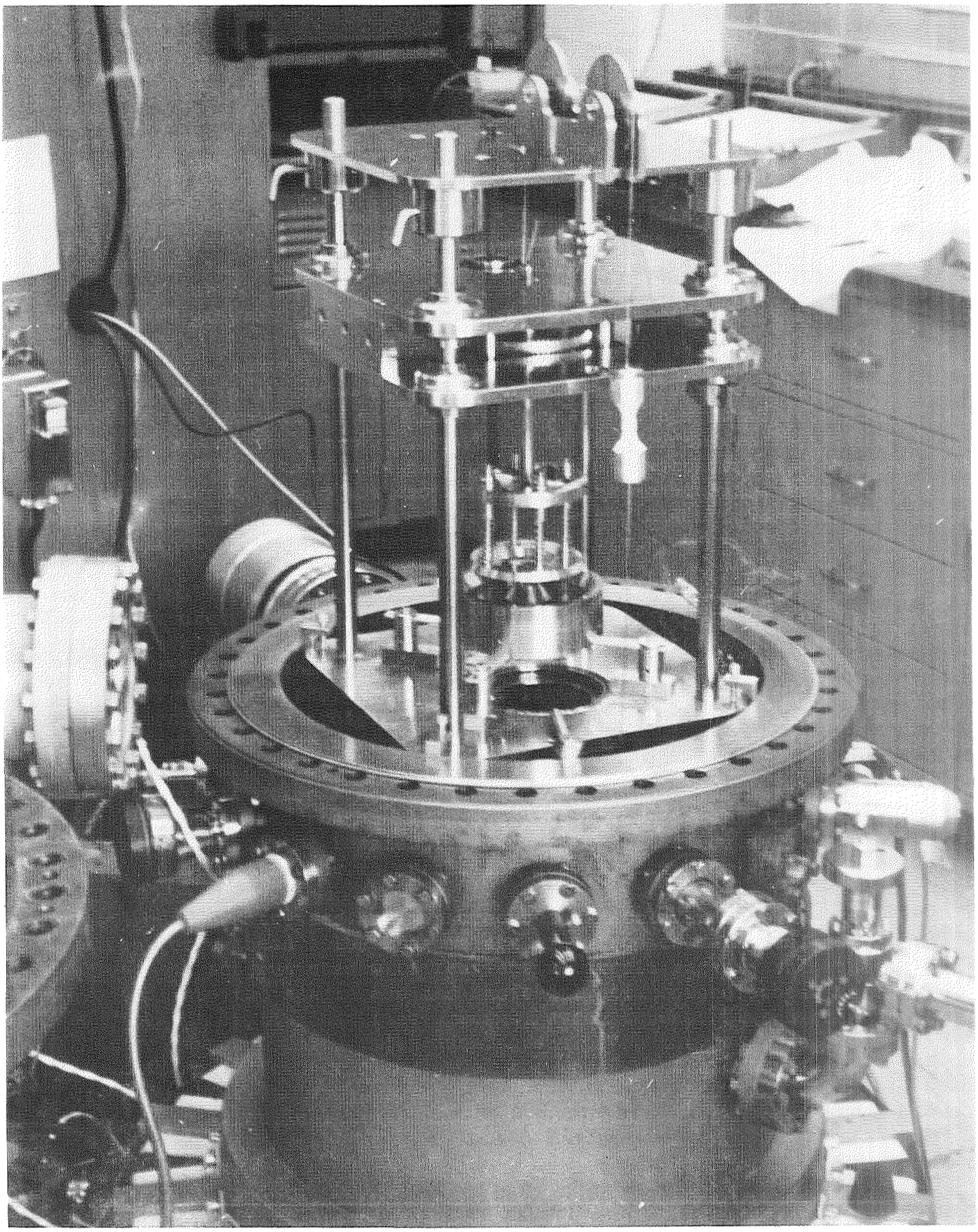

FIGURE 8. - Vacuum Torsional-Shear Tester (TCMRC).

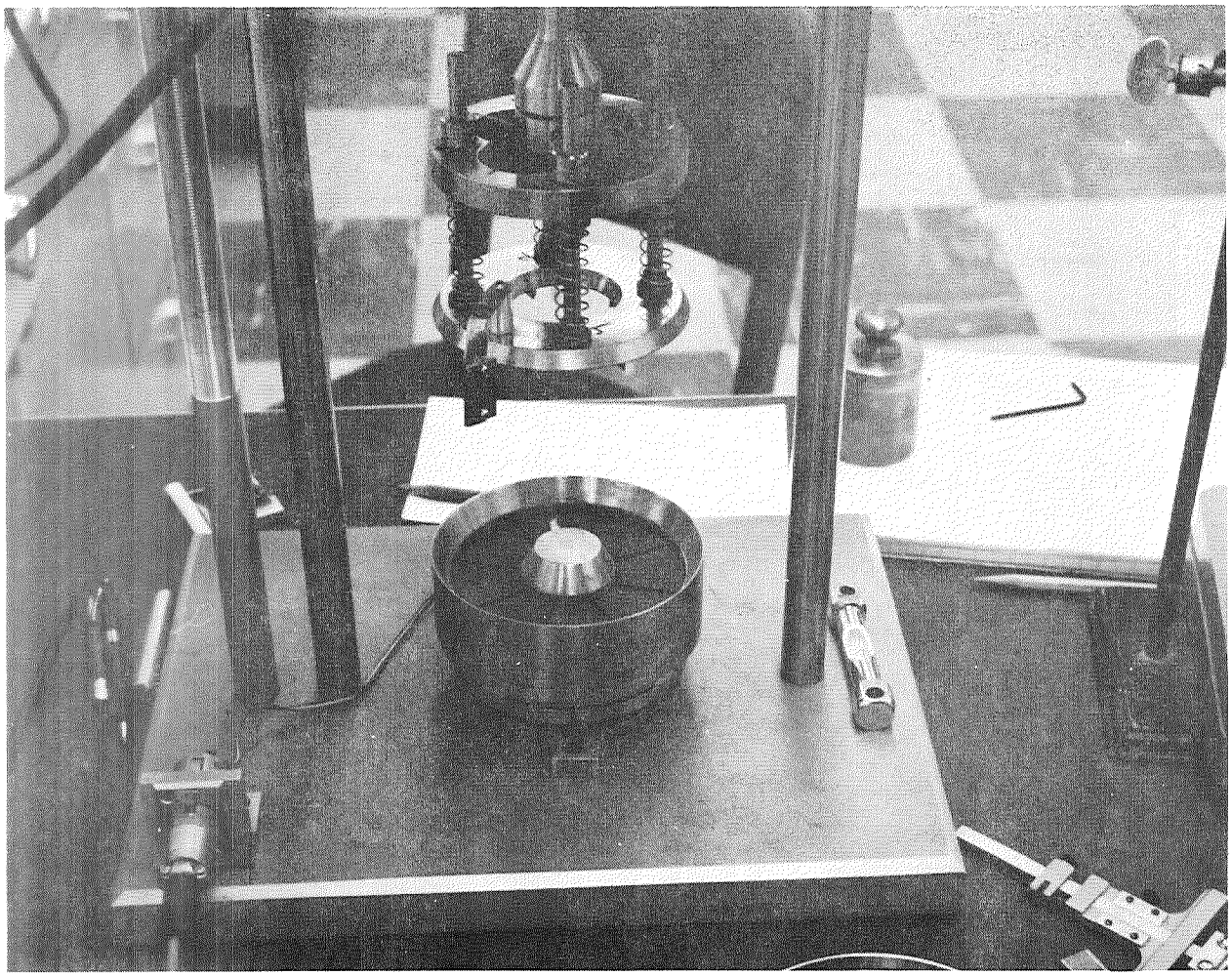

FIGURE 9. - Earth-Atmosphere Torsional-Shear Tester (SMRC).

For the automatic, continuous recording of the data, the normal load and shear-resistance transducer bridges are connected to a dual-channel, strain-gage recorder. Using deadweight loads, the bridges are calibrated on the recorder graph (fig. 10). Strain rates are calculated directly from the commercial gear-reduction factor of 1,800 to 1 by turning the vane drive at 1 rpm with a fractional-horsepower, shaded-pole motor. Strain rates at the center of mass distance are 0.016 cm/min, or approximately one-sixth of the rate normally used for shear testing of granular materials for terrestrial bin-flow studies. To record the strain, a microswitch, actuated by a cam on each revolution of the 1-rpm motor drive shaft, is connected to the time marker on the recorder. However, an alternate method of recording strain rate was to fix the recorder chart speed at 1 mm/min.

The principal deficiencies of the torsional-shear tester are the presence of friction at the chamber walls and the binding potential of particles wedged between the knife-edged vane head and the chamber wall. Further, the

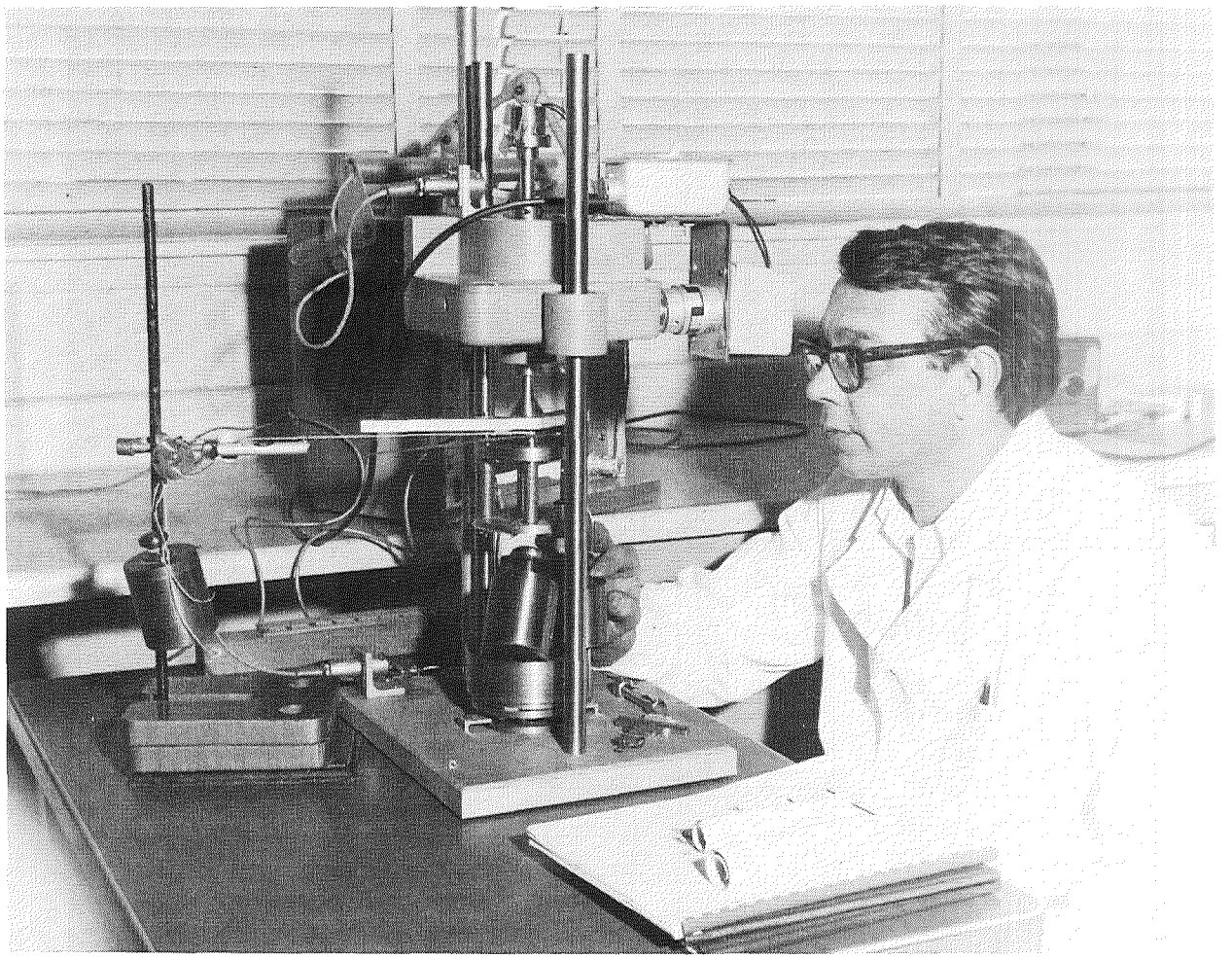

FIGURE 10. - Calibration of the Torsional-Shear Tester.

the consolidated basalt powder is treated as a solid cake which shears across the total sample surface, even though the vanes are inset from the chamber wall.

In preparation for a test, a 160-gram sample of basalt powder is oven dried at 110° C and cooled in a sealed desiccator until it reaches room temperature. The sample is placed loosely in the chamber, leveled, and measured with a depth gage, a procedure which obtains the initial density and void ratio. The loading head is pressed on the sample until a predetermined consolidation load is reached. The specimen remains under this load till consolidation is complete (about 1 hour with the simulated lunar soil). In the initial test the sample is sheared under a normal load equivalent to the preconsolidation load. It is allowed to shear through its peak strength to ultimate shear strength. The peak torsional shear values for these normally consolidated samples have been plotted in figure 5, whereas the ultimate strengths are plotted on the Jenike-type failure envelope. After shearing, the shear head is raised from the sample, and the height is measured to allow

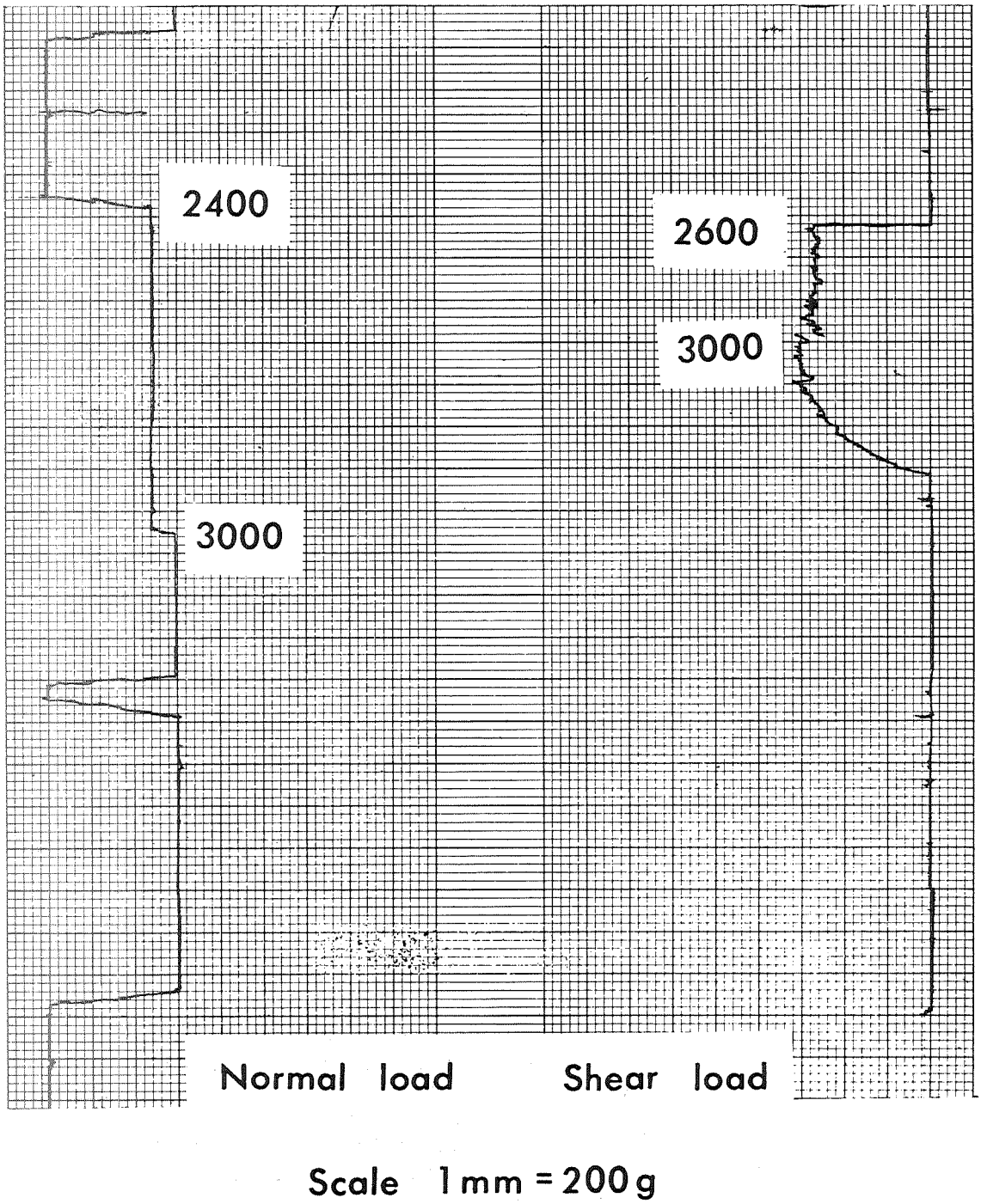

FIGURE 11. - Torsional Test Graph of Shear Load and Normal Load.

calculation of the final void ratio. Typical shear-test data, as recorded on the strain-gage recorder graph, are shown in figure 11.

The same sample is then remixed in the chamber, leveled with the depth gage, and consolidated under the same load. In this test, the normal load is reduced below that of the initial consolidation load, and the specimen again is sheared through the peak to ultimate strength. An identical procedure is repeated, at progressively reduced normal loads, as many times as necessary to obtain clear definition of the yield surface. In plotting the powder yield surface bin flow studies--as proposed by others (5, 7, 22)--the ultimate shear strength is used on the initial, normally consolidated shear test; whereas data from each subsequent test (with the normal load below the preconsolidation load) are based upon the peak shear-strength value obtained from the shear test. A yield surface is drawn through the points and extrapolated to the shear axis. A yield circle, to determine unconfined strength (f_c), is fitted under the extrapolated peak yield surface from the coordinate origin, and another circle is fitted graphically under the upper end of the surface to determine the principal consolidation stress (σ_1).[5] The ratio of the unconfined strength (f_c) over the principal yield stress (σ_1) is defined as the flow function (ff) of the material (5, 7), or

$$ff = \frac{\sigma_1}{f_c} . \qquad (1)$$

Another series of tests, at different consolidation loads, allow construction of a flow function for a granular material. Such a test series on the simulated lunar-soil matrix is shown in figures 12-14. A flow-function of lunar-soil matrix is plotted in figure 15, indicating a factor of about 6.5, which would classify the material as relatively easy-flowing, using Jenike's method of classification (7, p. 56). In fact, however, the basalt powder insofar as can be discerned from handling small quantities in flow hoppers and funnels in the laboratory, is rather difficult to manage and easily plugs in channels. Schramli (17) has reported similar difficulties in determining the flow properties of cement powders when simply defining their "flow functions." Other properties, discussed in the following section, could be equally as important to classification of the flowability of material as is the determination of unconfined strength and flow function.

The peak shear parameters for flow analysis used in part 2 of this paper are a Mohr envelope slope of 35-1/2° and adjusted cohesion (k) of 2 g/cm^2 or 0.028 psi, assuming that the effective cohesion will approach zero as incipient flow is reached.

One-Dimensional Compression Earth-Pressure-at-Rest Tests

A one-dimensional compression chamber was used to develop stress-strain properties and K_o stress ratios on the basalt powder. This Hendron-type, triaxial chamber (3) was originally constructed at the laboratory to perform high-pressure (2,000 psi) testing on mine backfills (12). Figure 16 is an assembly drawing of the chamber. It was modified for lunar-materials-handling studies

[5] It should be emphasized that this procedure of constructing Mohr's circles from the results of direct-shear tests is not generally practiced in soil mechanics.

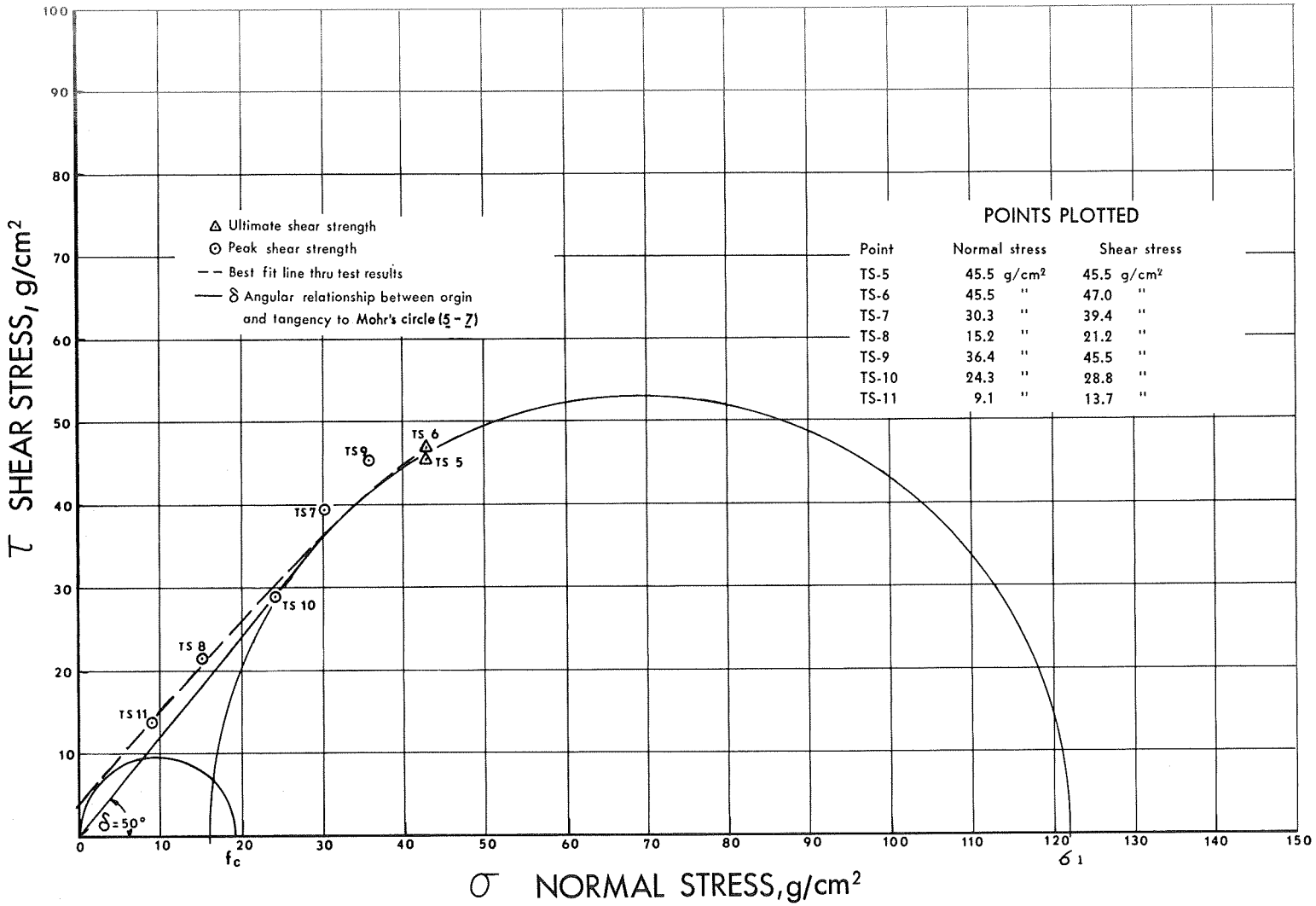
τ SHEAR STRESS, g/cm²
σ NORMAL STRESS, g/cm²
△ Ultimate shear strength
⊙ Peak shear strength
– – Best fit line thru test results
— δ Angular relationship between orgin and tangency to Mohr's circle (σ1 - σ3)
POINTS PLOTTED
Point | Normal stress | Shear stress
TS-5 | 45.5 g/cm² | 45.5 g/cm²
TS-6 | 45.5 " | 47.0 "
TS-7 | 30.3 " | 39.4 "
TS-8 | 15.2 " | 21.2 "
TS-9 | 36.4 " | 45.5 "
TS-10 | 24.3 " | 28.8 "
TS-11 | 9.1 " | 13.7 "
TS 5
TS 6
TS 7
TS 8
TS 9
TS 10
TS 11
δ = 50°
fc
σ1

FIGURE 12. - Results of Torsional-Shear Tests on Simulated Lunar Soil at 45.5 g/cm^2 Consolidation.

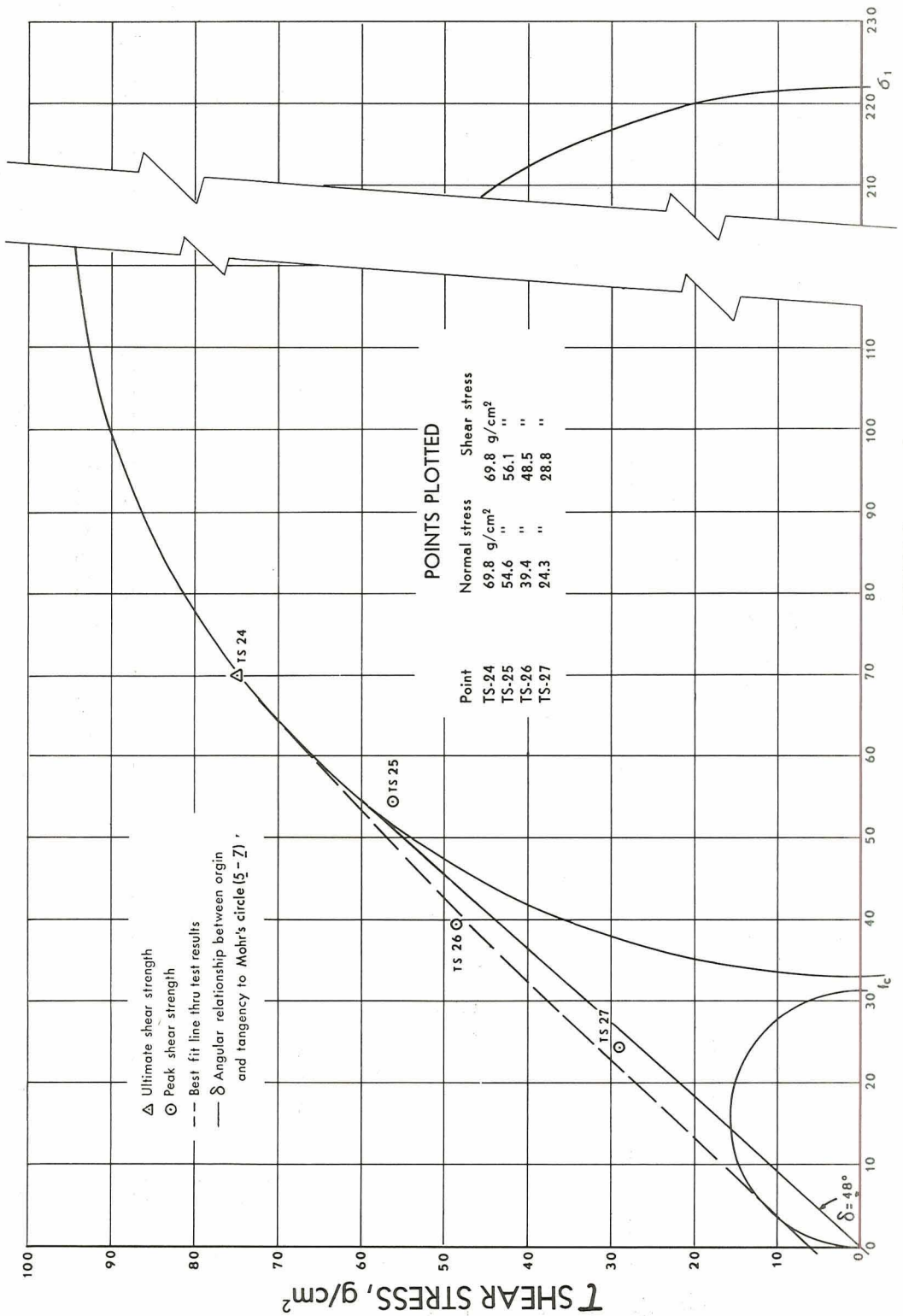
τ SHEAR STRESS, g/cm²
σ NORMAL STRESS, g/cm²
△ Ultimate shear strength
⊙ Peak shear strength
– – Best fit line thru test results
— δ Angular relationship between origin and tangency to Mohr's circle (5 – 7),
POINTS PLOTTED
Point | Normal stress | Shear stress
TS-24 | 69.8 g/cm² | 69.8 g/cm²
TS-25 | 54.6 " | 56.1 "
TS-26 | 39.4 " | 48.5 "
TS-27 | 24.3 " | 28.8 "
TS 24
TS 25
TS 26
TS 27
δ = 48°
σ1
σc

FIGURE 13. - Results of Torsional-Shear Tests on Simulated Lunar Soil at 69.8 g/cm^2 Consolidation.

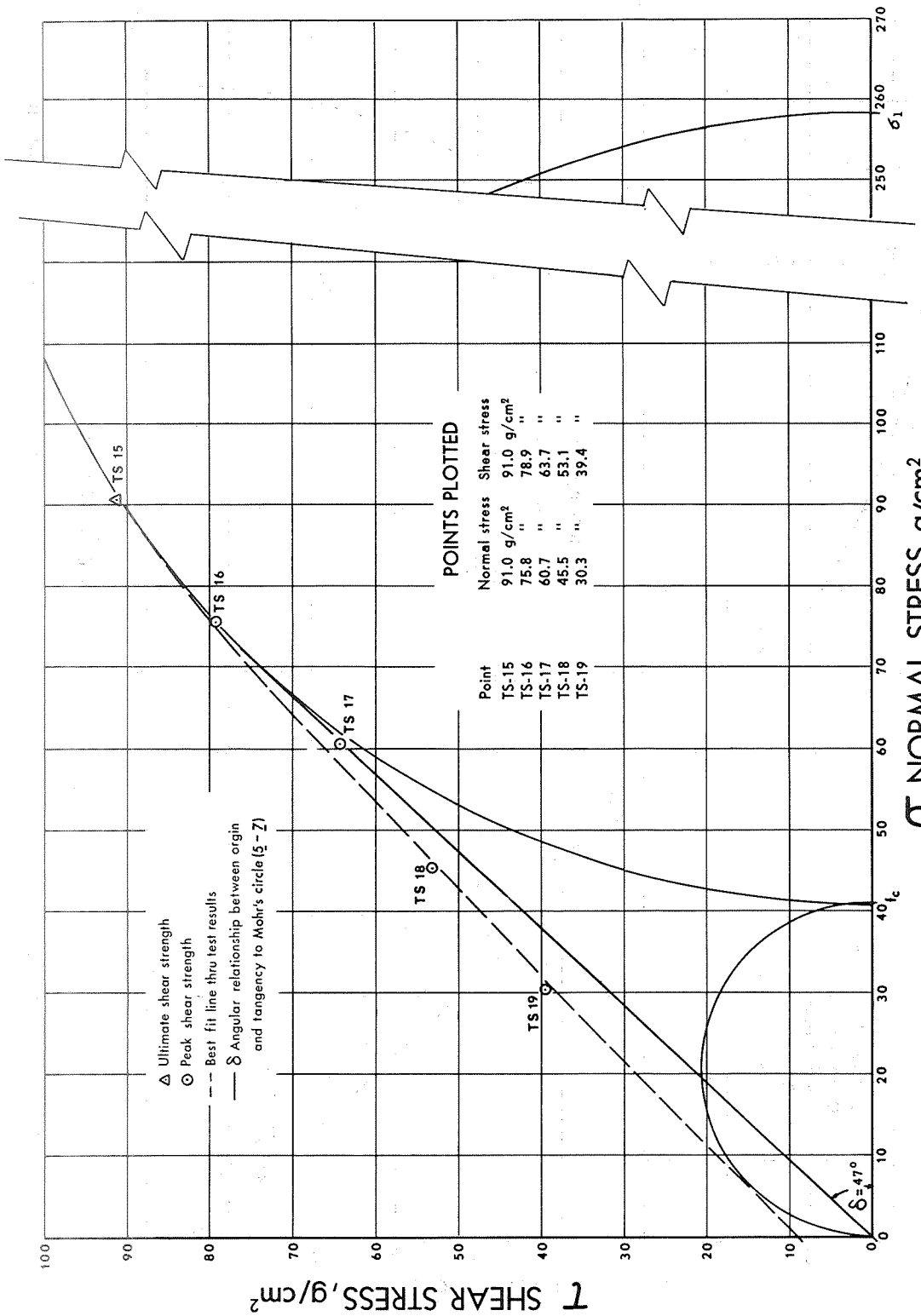

FIGURE 14. - Results of Torsional-Shear Tests on Simulated Lunar Soil at 91.0 g/cm^2 Consolidation.

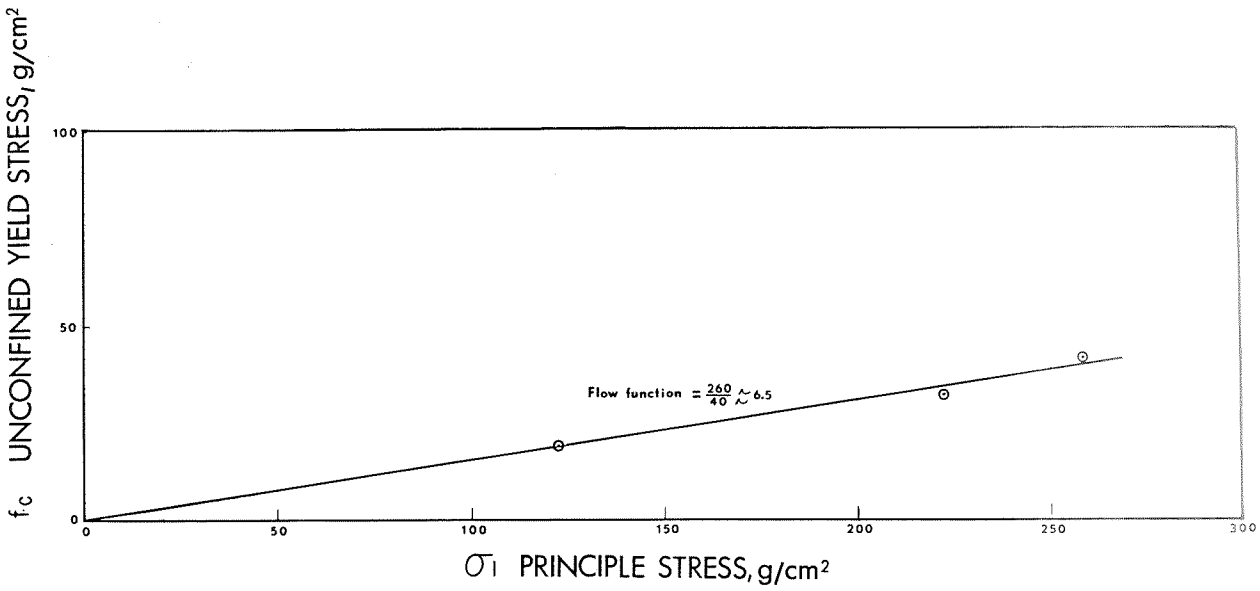

FIGURE 15. - Flow-Function of Simulated-Soil Matrix From Torsional-Shear Tests.

to record pressures in the 100-psi range. A 10-psi range would have been preferable for this testing, but at the time there was no reliable way to increase the sensitivity of the chamber.

The sample chamber wall is a 0.09-inch-thick steel sleeve, on whose outer wall are mounted three independent strain-gage bridges. Figure 17 displays the base plate, chamber housing, and sidewall sleeve prior to assembly. Each strain-gage bridge consists of two active gages on the wall sleeve and two dummy gages mounted on a floating steel block. Hydraulic oil surrounds the outer wall of the sleeve. When the sample is tested, the vertical stress (σ_1) applied by the loading head causes lateral strain, and oil pressure is applied to the system to null the bridge--and thereby nullify the lateral strain in the sample. A pressure transducer and a visual pressure gage serve to record the lateral stress (σ_h).

From the tests, exact values of the coefficient of earth-pressure-at-rest (K_o) can be obtained:

$$K_o = \frac{\sigma_h}{\sigma_v} \qquad (2)$$

σ_h = lateral horizontal stress.

σ_v = applied vertical stress.

This coefficient is less constant than generally assumed; for it depends on the void ratio or packing state of the material and, most significantly, on its stress history, as Hendron (3) deduced from his work on cohesionless sands (fig. 18), and as is corroborated by other soil-mechanics work discussed by

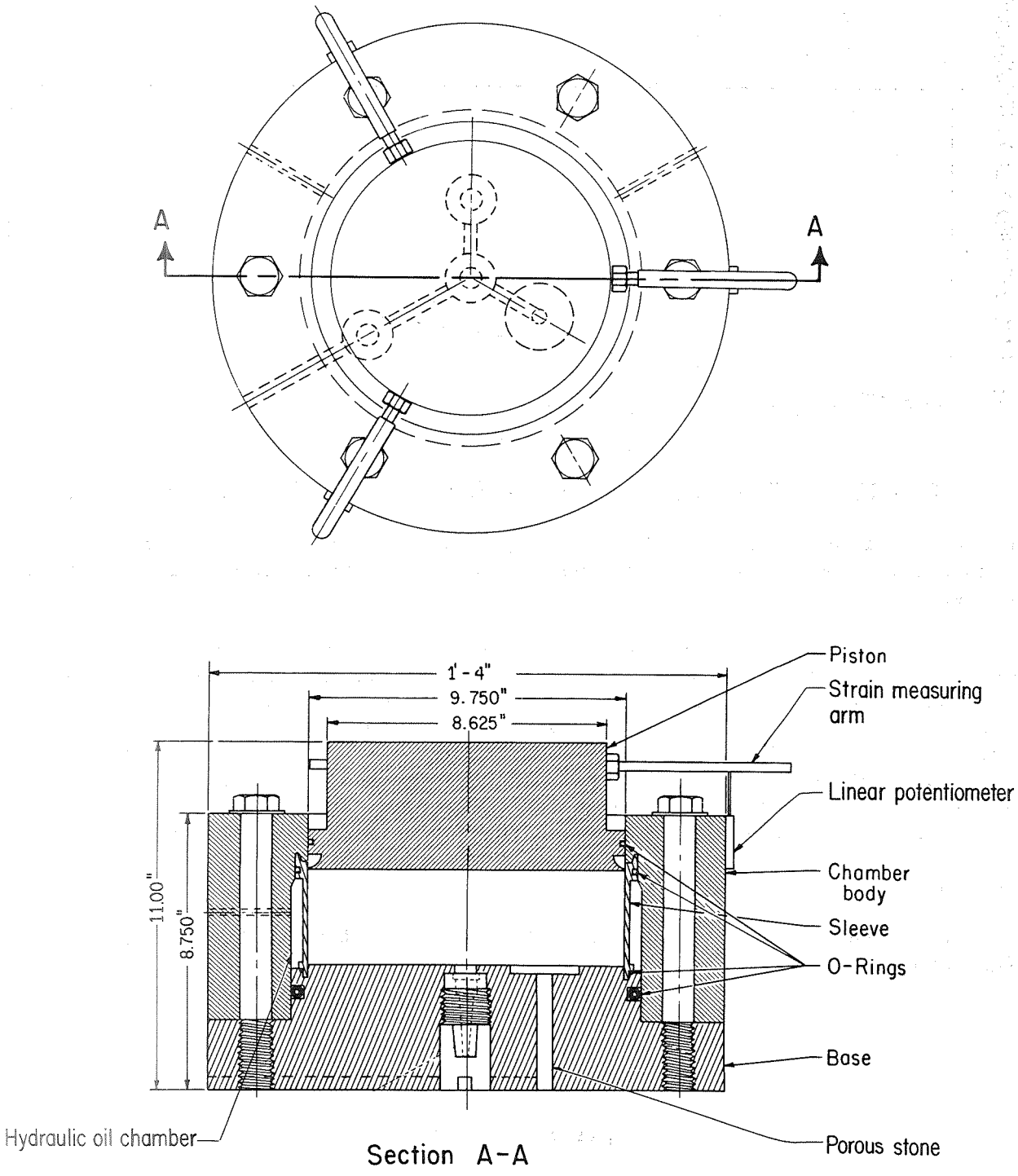

FIGURE 16. - One-Dimensional Compression K_o Chamber.

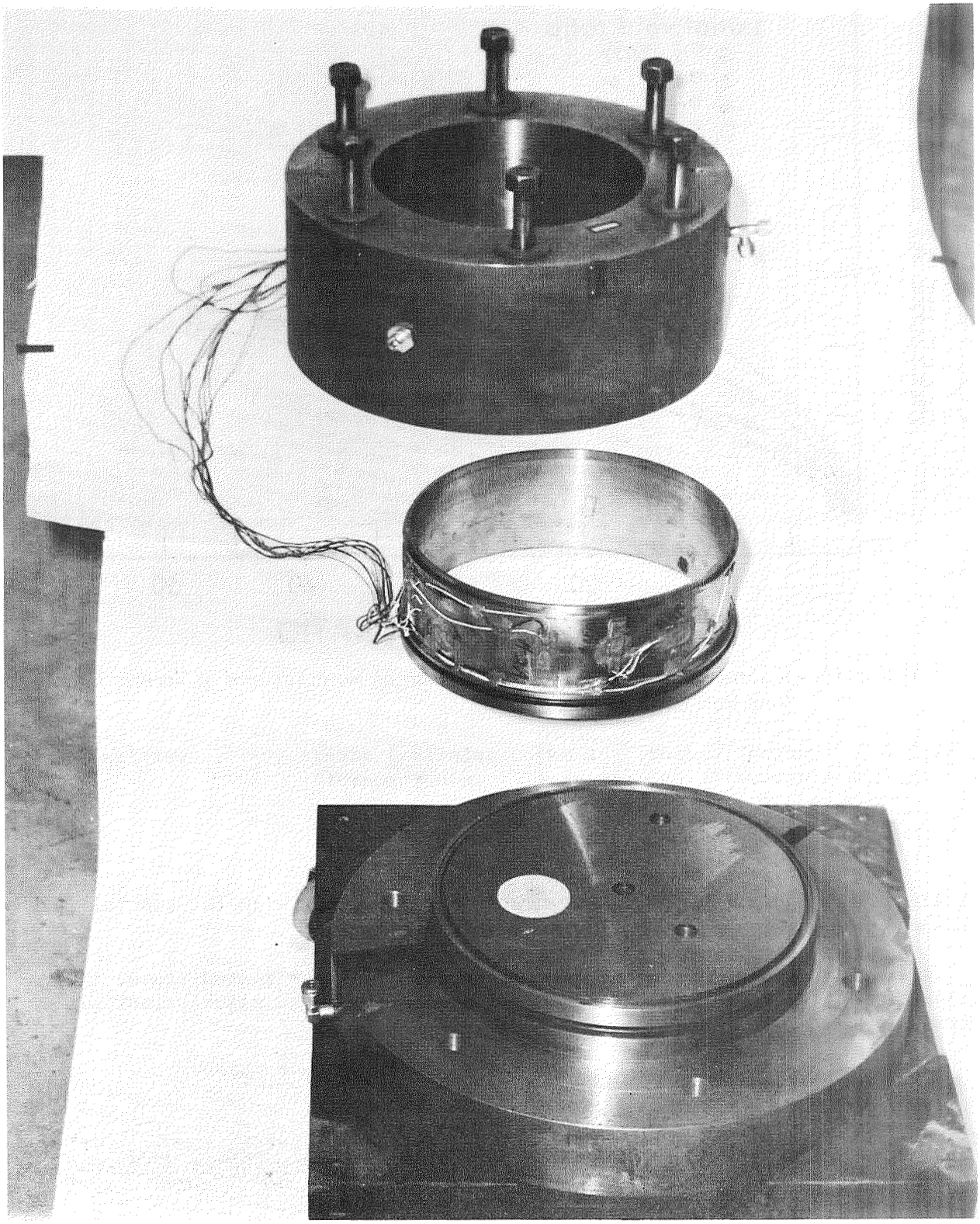

FIGURE 17. - K_o Chamber Prior to Assembly.

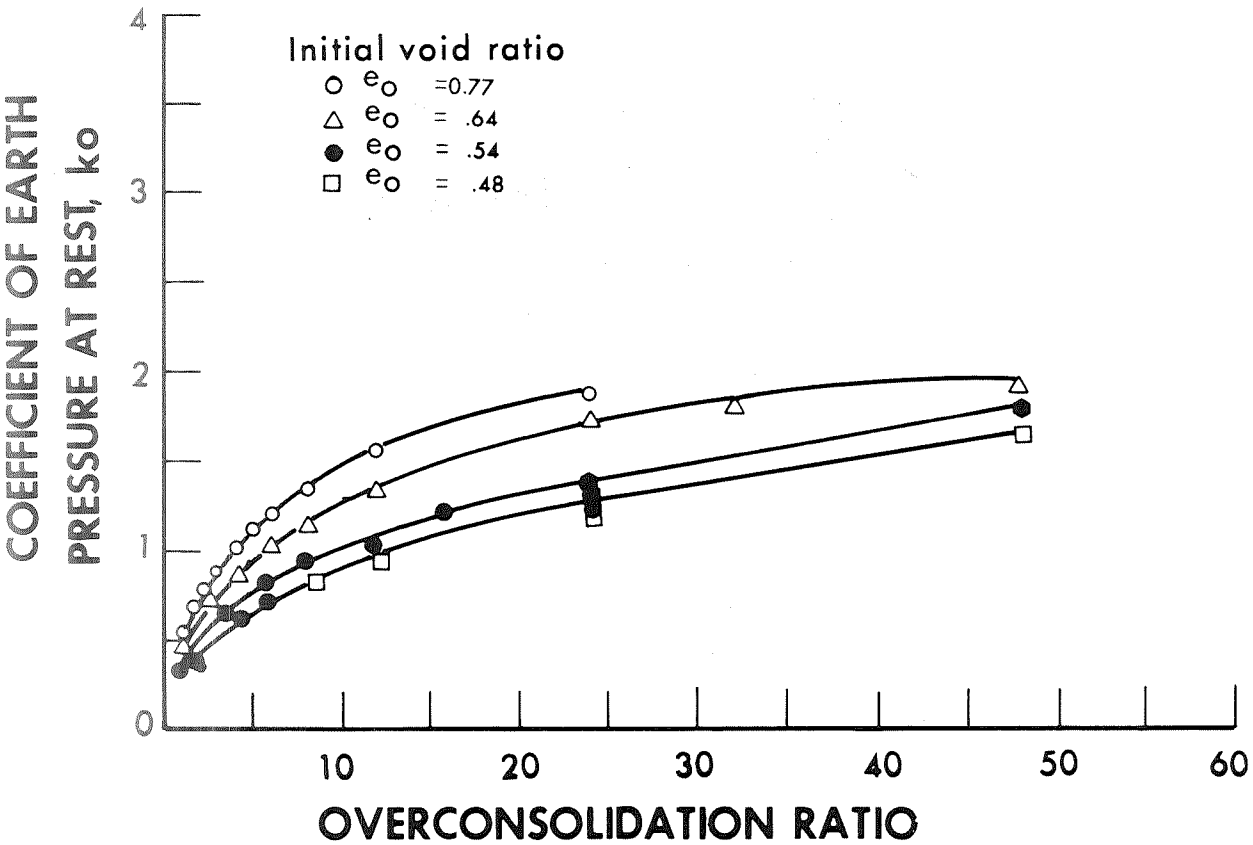

FIGURE 18. - K_o Stress Ratio Versus Overconsolidation Ratio for Sand at Various Initial Void Ratios (After Hendron).

Henkel (4). During loading, the major principal stress (σ_1) is vertical, whereas the minor principal stress (σ_3) is horizontal.

$$K_o = \frac{\sigma_3}{\sigma_1} < 1. \tag{3}$$

Equation 3 is indicative of the at-rest stress in a bin with the control gate closed.

During unloading, with the material in an overconsolidated state, the K_o value is seen to rise, and the lateral stress becomes the major principal stress:

$$K_o = \frac{\sigma_1}{\sigma_3} \longrightarrow \text{Kp (Rankine's coefficient of passive earth pressure).} \tag{4}$$

Equation 4 represents a stress state that might be present in a gravity-flow bin after the control gate has been opened and the bulk material approaches incipient flow.

Both of these concepts are not only at variance with the common procedure of predicating a Rankine active-pressure relation to define the stress field in a gravity bin, but also with Jenike's use of a uniform radial stress field near the discharge point in a flowing bin.

To develop a modulus of deformation (M) (secant modulus), an accurate measurement of the induced strain and applied stress was made. Strain in the sample was recorded by three linear potentiometers, which are mounted on the outside of the chamber housing. For ascertaining the applied load, a turn-potentiometer is mounted on the strain-controlled universal testing machine. Further, for observation of stress distribution in the chamber, three small pressure transducers are mounted in both the loading head and base plate. Figure 19 pictures the assembled chamber and a data-acquisition system.

In each test, a sample was placed in the chamber in a loose state and carefully leveled and measured. The loading head was lowered onto the sample by the universal testing machine. At this point, all stress-strain instrumentation was balanced and zeroed out, and the initial no-load readings were recorded on both printed and punched tape. In each compression test, a 1-psi load was applied and then raised in 10- or 20-psi increments at a head-displacement rate of 0.025 in/min. At each load increment, the multichannel scanner monitored the 13 channels of stress-strain instrumentation, and simultaneously the data-acquisition system produced a printed tape and punch-tape record of each circuit output. Throughout the test, one of the three strain-gage bridges on the steel sidewall sleeve was monitored on a strain indicator; it was kept in a null or no-strain position by the application of hydraulic pressure with a hand pump. During testing, both the load and unload portions of the virgin compression cycle (fig. 20) were observed. (Two additional hysteresis loops were also performed on each sample, but only the initial virgin loop is presently of interest.) The secant modulus (M) of the powder material is determined from the stress-strain measurements, and the K_o stress ratio values are used to calculate a Poisson's ratio (μ) for the material (18):

$$\mu = \frac{K_o}{K_o + 1} . \tag{5}$$

Therefore, the two significant parameters generated by the one-dimensional compression tests can be incorporated into a finite-element mesh of a representative bin filled with the bulk-powder material, and can accurately define the properties of each element in the mesh. Under conditions of loading the constrained modulus M is used, while for unloading, an unconstrained E modulus value is calculated for the material, as shown in the appendix.

An example of results from the one-dimensional compression tests performed on the simulated lunar soil is shown in table 2. The complete initial-compression cycle at all load increments and the physical-property parameters under discussion are included in the table. With initial loading of the powder sample, and the OCR (overconsolidation ratio) being equal to 1, the K_o ratio has a value of about 0.3. After the reduction of the load to 1 psi (and with a large OCR), the residual K_o value in the simulated lunar soil exceeds

2.0, at which point it is approaching the value of the passive earth pressure coefficient of the simulated lunar soil.

TABLE 2. - Earth-pressure-at-rest compression tests on simulated lunar soil

Total applied stress (σ_v), psi	Total lateral stress (σ_h), psi	Total strain vertical (ε_v), in/in	Void ratio (e)	Secant modulus (M), psi	Coeff. of earth press. at rest (K_o)	Poisson's ratio (μ)	Overconsolidation ratio (OCR)
0.0	0.0	0.0000	1.0092	0.0	0.0000	0.0000	1.00
1.0	.7	.05661	.8955	17.3	-	-	1.00
20.3	7.3	.11389	.7804	177.8	.3610	.2652	1.00
39.7	13.8	.12512	.7579	317.1	.3480	.2582	1.00
59.5	20.8	.13218	.7437	450.5	.3494	.2589	1.00
80.4	27.3	.13760	.7328	584.4	.3390	.2532	1.00
100.3	34.1	.14172	.7245	707.7	.3398	.2538	1.00
120.1	40.3	.14517	.7176	827.0	.3354	.2511	1.00
139.8	46.8	.14802	.7118	944.2	.3348	.2508	1.00
119.4	41.6	.14809	.7117	806.0	.3483	.2583	1.17
100.1	35.7	.14801	.7119	676.6	.3569	.2630	1.40
80.3	29.8	.14778	.7123	543.3	.3712	.2707	1.74
60.0	24.4	.14734	.7132	407.2	.4068	.2892	2.33
40.2	18.9	.14701	.7139	273.4	.4695	.3195	3.48
20.1	12.0	.14606	.7158	137.7	.5988	.3745	7.00
1.0	2.1	.14313	.7217	6.9	2.1547	.6830	140.00
1.0	1.8	.14290	.7221	6.8	1.8627	.6507	140.00

For comparative testing, a coarser, more uniform basalt powder was prepared, by ball-mill grinding, from the same basalt rocks used to produce the impact-milled, lunar-soil material. Direct shear tests run on ball-milled basalt powder indicate a peak angle of internal friction $\phi = 40°$ and cohesion intercept (c) of about 50 g/cm^2. These figures are slightly greater than the peak friction and cohesion parameters determined for the impact-milled basalt powder illustrated in figure 5. Interestingly, when the two powders are tested in a laboratory flow-cone, the ball-milled basalt powder possesses consistent and easy-flowing properties, whereas the impact-milled basalt powder plugs and produces erratic flow from the cone, even though the basalt powders have similar shear-strength properties. However, a one-dimensional compression test performed on the ball-milled basalt powder indicates a reduced residual K_o value of only 1.3 at the final OCR, whereas the impact-milled basalt powder residual K_o value exceeds 2.0, as previously shown in table 2. Thus, it is postulated that residual stresses in these two basalt powders--not their relative shear strengths--create the wide divergence in their flow properties.

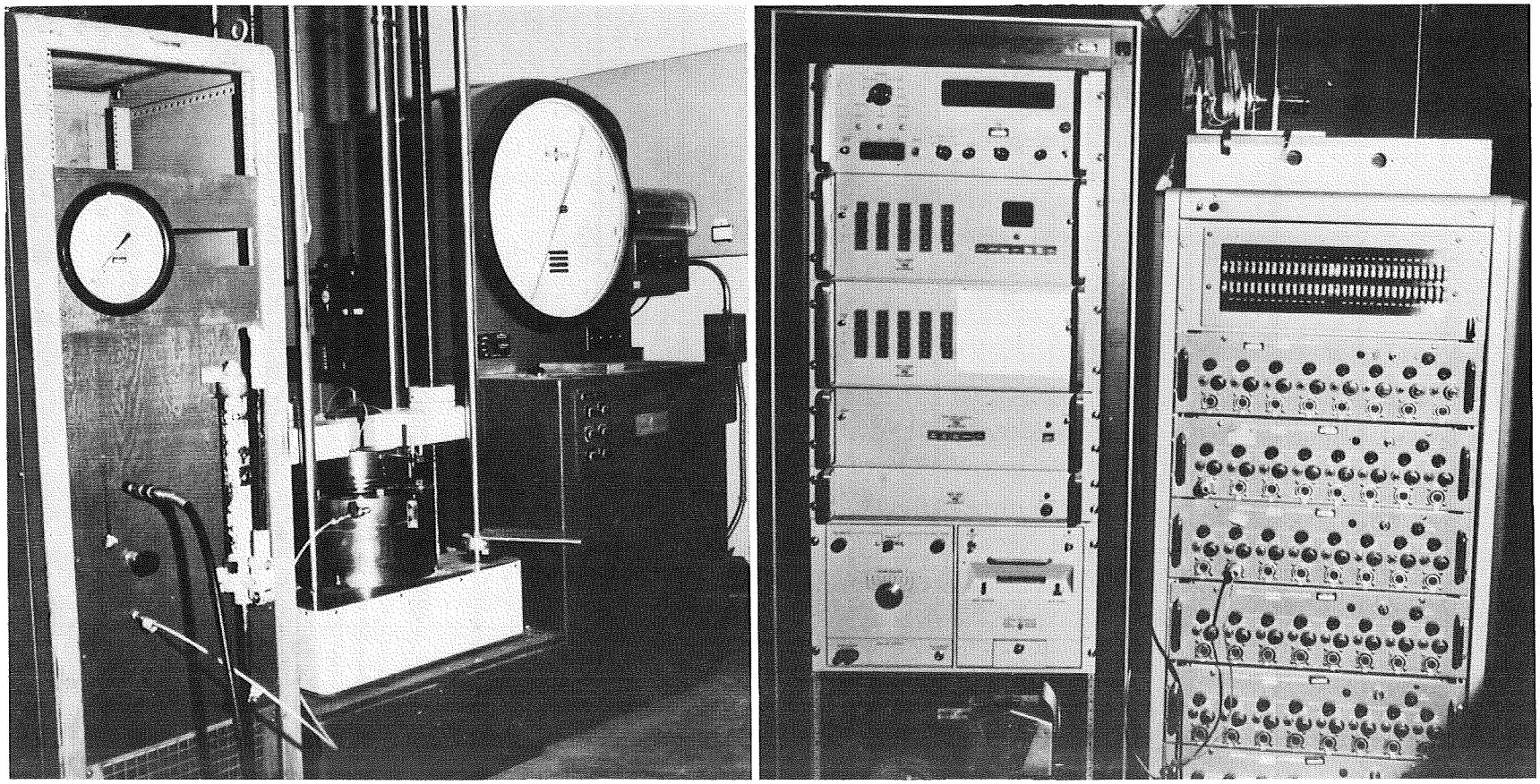

FIGURE 19. - K_o Chamber and Data-Acquisition System.

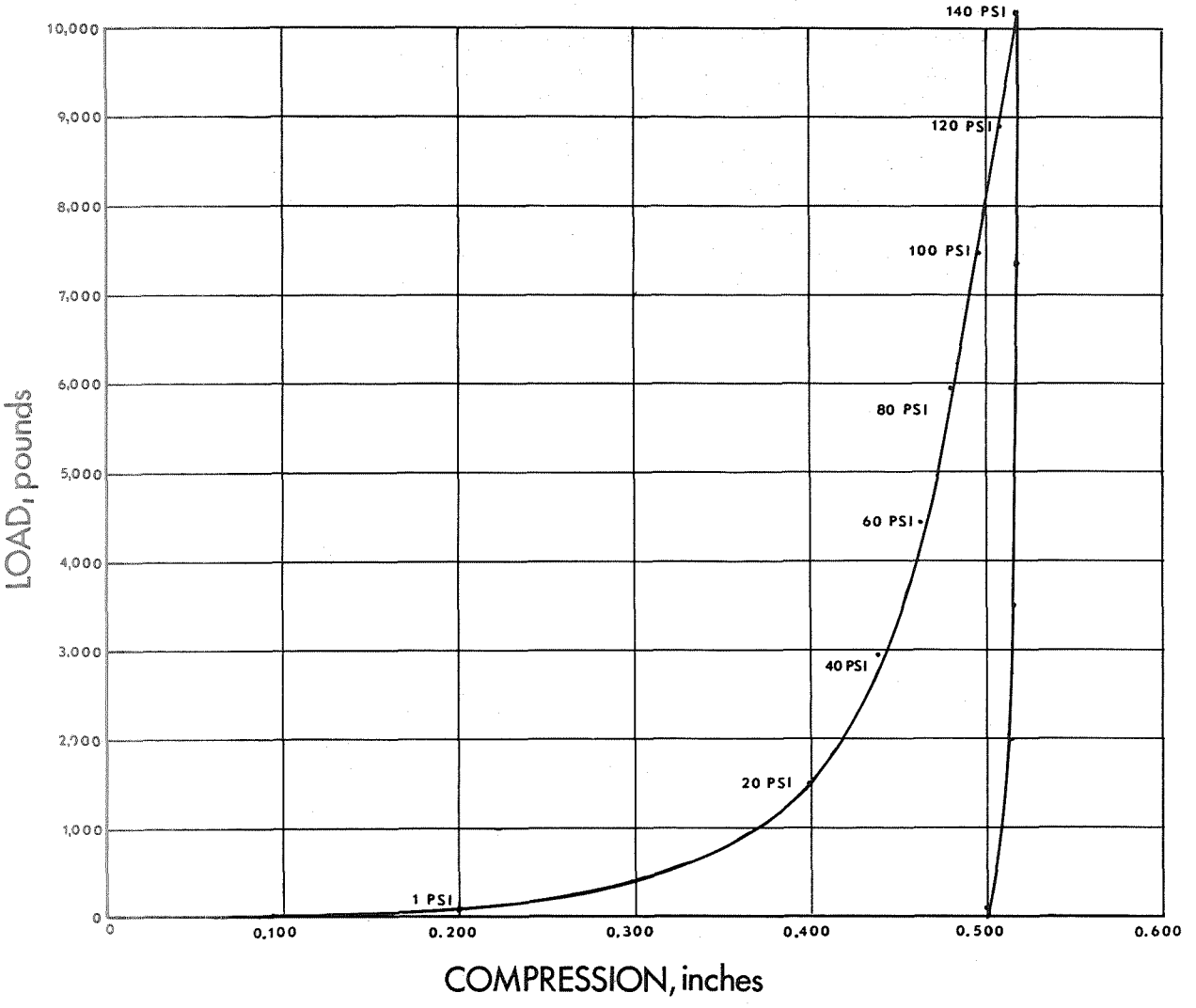

FIGURE 20. - Load-Displacement Curve for Simulated Lunar Soil From K_o Compression Test.

SUMMARY AND CONCLUSIONS

This research work--to develop a simple method of designing gravity-flow bins for lunar-support operations--has adapted several new, though well-developed, testing methods for studying the gravity flow of powder materials. An analysis of gravity-flow of lunar-powder material by finite-element techniques has been herein proposed. It is submitted that much of this research is applicable to common gravity-flow bin design in industries handling bulk solids and powders.

A simulated lunar-soil powder was developed by impact crushing. The mechanical properties of this powder correlate closely with those predicted for the in situ lunar soil.

Direct-shear tests were performed to define a peak-strength Mohr failure envelope, as well as to provide a linear Mohr failure criterion for the lunar material selected for finite-element analysis. A torsional-shear device, similar to the Walker ring shear tester, was developed principally for testing in an ultrahigh vacuum system. The prototype torsional-shear tester has provided a simplified procedure, in that a sample can be sheared through its peak to ultimate shear in a single continuous test.

A one-dimensional compression chamber was used to define the deformation modulus (M) and the K_o stress ratio value of the simulated lunar soil, which can be utilized in a finite-element solution of gravity flow. Of particular interest in the K_o testing was the observation that residual lateral stresses become proportionally higher when the basalt powder is unloaded. It is postulated that these increases in the K_o stress-ratio value are indicative of the stresses present in a bin when the basalt powder material approaches incipient flow. Further, the increases in K_o value--which vary with void ratio, overconsolidation ratio, and other mechanical properties--could provide an alternate method of rating the flowability of bulk solids or powders which do not lend themselves to other types of analysis (17). Finally, development of a more sensitive, lower-pressure K_o chamber would seem warranted. Testing then could be performed in a load range more representative of common bin loads; the powder would be less compressed; and higher residual K_o stresses could be expected at lesser overconsolidation ratios.

REFERENCES

1. Atchison, T. C., and C. W. Shultz. Bureau of Mines Research on Lunar Resource Utilization. Proc. of Working Group on Extraterrestrial Resources, NASA SP-177, February 1968, pp. 65-74.

2. Fogelson, D. E. Simulated Lunar Rocks. Proc. of the Working Group on Extraterrestrial Resources, NASA SP-177, February 1968, pp. 75-95.

3. Hendron, A. J. The Behavior of Sand in One-Dimensional Compression (Ph. D. Thesis, University of Illinois). University Microfilms, Inc., Ann Arbor, Mich., 1963, 283 pp.

4. Henkel, D. J. Geotechnical Considerations of Lateral Stress. Lateral Stress in the Ground and Design of Earth-Retaining Structures Conf., ASCE, New York, 1970, pp. 1-50.

5. Jenike, A. W. Gravity Flow of Bulk Solids. Bull. 108, Univ. of Utah, v. 52, No. 29, October 1961, 309 pp.

6. _____. Storage and Flow of Solids. Trans. Soc. Min. Eng., AIME, v. 235, September 1966, pp. 267-276.

7. _____. Storage and Flow of Bulk Solids. Bull. 123, Univ. of Utah, v. 52, No. 26, November 1964, 198 pp.

8. Jenike, A. W., and T. Leser. A Flow No-Flow Criterion in the Flow of Powder in Converging Channels. Fourth Internat. Cong. on Rheology, Brown Univ., August 1963, pp. 125-141.

9. National Aeronautics and Space Administration. Surveyor VI Preliminary Rept. NASA SP-166, May 1968, 168 pp.

10. _____. Apollo-11 Preliminary Science Rept. NASA SP-214, October 1969, 203 pp.; American Association for Advancement of Science. V. 167, No. 3918, Jan. 30, 1970, pp. 447-790.

11. _____. Apollo-12 Preliminary Science Rept. NASA SP-235, June 1970, 227 pp.

12. Nicholson, D. E., and R. Busch. Earth Pressure at Rest and One-Dimensional Compression in Mine Hydraulic Backfills. BuMines Rept. of Inv. 7198, October 1968, 40 pp.

13. Nicholson, D. E., and H. Pettibone. Status Report on the Fine-Particle Project. (BuMines/NASA Unpublished Rept.) Spokane Mining Research Center, January 1968, 15 pp.

14. Palmer, L. A., P. Brown, and C. M. Yeomans. A Procedure for Separately Evaluating Friction and Cohesion of Soils by a Consolidated Direct-Shear Test. ASTM Special Tech. Pub. No. 206, Am. Soc. for Testing and Materials, Philadelphia, Pa., October 1957, pp. 34-44.

15. Roepke, W. W. Friction Tests in Simulated Lunar Vacuum. Proc. of the Working Group on Extraterrestrial Resources, NASA SP-229, June 1969, pp. 107-112.

16. Roscoe, K. H., A. N. Schofield, and C. H. Wroth. On Yielding of Soils. Geotechnique, No. 8, 1958, pp. 22-58.

17. Schramli, W. On Measurements of Flow Properties of Cement. Powder Technol., v. 1, No. 4, December 1967, pp. 221-227.

18. Terzaghi, Karl. Theoretical Soil Mechanics. John Wiley & Sons, Inc., New York, 9th ed., 1943, 510 pp.

19. Tschebotarioff, Gregory P. Soil Mechanics, Foundations, and Earth Structures. McGraw-Hill Co., Inc., New York, 1951, 655 pp.

20. Walker, D. M. An Approximate Theory for Pressures and Arching in Hoppers. Chem. Eng. Sci., v. 21, 1966, pp. 975-997.

21. _____. A Basis for Bunker Design. Powder Technol., v. 1, No. 4, December 1967, pp. 228-236.

22. Williams, J. C., and A. Birks. The Preparation of Powder Specimens for Shear Testing. Rheologica Acta., v. 3, May 1965, pp. 170-180.

23. Zienkiewicz, O. C., and Y. K. Cheung. The Finite-Element Method in Structural and Continuum Mechanics. McGraw-Hill Co., Inc., New York, 1967, 274 pp.

APPENDIX

Conversion of the "constrained" modulus, M, to "unconstrained" modulus, E, for the powder after the orifice has been opened and incipient flow approached is performed in the following example.

By polar coordinates:

$$E\epsilon_z = \sigma_z - \mu(\sigma_r + \sigma_\theta) \tag{A-1}$$

$$E\epsilon_r = \sigma_r - \mu(\sigma_z + \sigma_\theta) \tag{A-2}$$

$$E\epsilon_\theta = \sigma_\theta - \mu(\sigma_z + \sigma_r). \tag{A-3}$$

By definition of the one-dimensional compression test $\epsilon_r = o$ and $\epsilon_\theta = o$, therefore,

$$\sigma_r = \mu(\sigma_\theta + \sigma_z)$$

$$\sigma_\theta = \mu(\sigma_r + \sigma_z)$$

$$\sigma_r = \sigma_\theta = \frac{\mu}{1-\mu}\sigma_z$$

substituting in equation A-1:

$$E\epsilon_z = \sigma_z - 2\mu\left(\frac{\mu}{1-\mu}\sigma_z\right)$$

$$= \sigma_z\left(1-2\mu\left(\frac{\mu}{1-\mu}\right)\right)$$

$$= \sigma_z\,\frac{(1-\mu-2\mu^2)}{1-\mu}$$

therefore,

$$\frac{\sigma_z}{\epsilon_z} = E\frac{(1-\mu)}{(1-\mu-2\mu^2)}$$

By definition $\frac{\sigma_z}{\epsilon_z}$ = M modulus from test.

Therefore,

$$E = M\,\frac{(1-\mu-2\mu^2)}{1-\mu}\,.$$

INT.-BU.OF MINES,PGH.,PA. 16425